NeuroImage: Clinical 30 (2021) 102583

Contents lists available at ScienceDirect

NeuroImage: Clinical

journal homepage: www.elsevier.com/locate/ynicl

Gray matter abnormalities follow non-random patterns of co-alteration in autism: Meta-connectomic evidence

Donato Liloia [a,b], Lorenzo Mancuso [a,b], Lucina Q. Uddin [c,d], Tommaso Costa [a,b,e,*], Andrea Nani [a,b], Roberto Keller [f], Jordi Manuello [a,b], Sergio Duca [a,b], Franco Cauda [a,b,e]

[a] GCS-fMRI, Koelliker Hospital and Department of Psychology, University of Turin, Turin, Italy
[b] Functional Neuroimaging and Complex Neural Systems (FOCUS) Laboratory, Department of Psychology, University of Turin, Turin, Italy
[c] Department of Psychology, University of Miami, Coral Gables, FL, USA
[d] Neuroscience Program, University of Miami Miller School of Medicine, Miami, FL, USA
[e] Neuroscience Institute of Turin (NIT), Turin, Italy
[f] Adult Autism Center, DSM Local Health Unit, ASL TO, Turin, Italy

ARTICLE INFO

Keywords:
Autism spectrum disorder
Activation likelihood estimation
Connectome
Anatomical covariance
Graph analysis
Diffusion tensor imaging

ABSTRACT

Background: Autism spectrum disorder (ASD) is a neurodevelopmental disorder characterized by atypical brain anatomy and connectivity. Graph-theoretical methods have mainly been applied to detect altered patterns of white matter tracts and functional brain activation in individuals with ASD. The network topology of gray matter (GM) abnormalities in ASD remains relatively unexplored.

Methods: An innovative *meta*-connectomic analysis on voxel-based morphometry data (45 experiments, 1,786 subjects with ASD) was performed in order to investigate whether GM variations can develop in a distinct pattern of co-alteration across the brain. This pattern was then compared with normative profiles of structural and genetic co-expression maps. Graph measures of centrality and clustering were also applied to identify brain areas with the highest topological hierarchy and *core* sub-graph components within the co-alteration network observed in ASD.

Results: Individuals with ASD exhibit a distinctive and topologically defined pattern of GM co-alteration that moderately follows the structural connectivity constraints. This was not observed with respect to the pattern of genetic co-expression. Hub regions of the co-alteration network were mainly left-lateralized, encompassing the precuneus, ventral anterior cingulate, and middle occipital gyrus. Regions of the default mode network appear to be central in the topology of co-alterations.

Conclusion: These findings shed new light on the pathobiology of ASD, suggesting a network-level dysfunction among spatially distributed GM regions. At the same time, this study supports pathoconnectomics as an insightful approach to better understand neuropsychiatric disorders.

1. Introduction

Autism spectrum disorder (ASD) is the diagnostic label that refers to a set of neurodevelopmental conditions characterized by impairment in social abilities, repetitive behaviors, restricted interests and abnormal sensory processing (American Psychiatric Association, 2013). This cluster of conditions reports clinical features persisting throughout the lifespan (Brighenti et al., 2018; Keller et al., 2020; Lord et al., 2018) and afflicting approximately 1 in 54 children aged 8 years (Baio et al., 2018).

Over the past decades, neuroimaging studies have suggested that ASD is associated with both anatomical and functional brain abnormalities (for a review see Ecker et al., 2015). In particular, voxel-based morphometry (VBM), a univariate technique capable of quantifying morphometric differences between diagnostic groups (Ashburner and Friston, 2000), has been used extensively to elucidate the neuroanatomy of autism. In addition, coordinate-based *meta*-analyses (CBMAs) have identified concordant structural effects across independent ASD studies, showing focal aberrations in multiple areas such as the cerebellum,

* Corresponding author at: Department of Psychology, Via Giuseppe Verdi 10, 10124 Turin, Italy.
E-mail addresses: donato.liloia@unito.it (D. Liloia), lorenzo.mancuso@unito.it (L. Mancuso), l.uddin@miami.edu (L.Q. Uddin), tommaso.costa@unito.it (T. Costa), andrea.nani@unito.it (A. Nani), rokel2003@libero.it (R. Keller), jordi.manuello@unito.it (J. Manuello), ducasergio@osp-koelliker.it (S. Duca), franco.cauda@unito.it (F. Cauda).

https://doi.org/10.1016/j.nicl.2021.102583
Received 28 October 2020; Received in revised form 15 December 2020; Accepted 30 January 2021
Available online 12 February 2021

amygdala-hippocampus complex, cingulate cortex, parieto-occipital pole, temporal and prefrontal cortices (Carlisi et al., 2017; Cauda et al., 2014, 2011; DeRamus and Kana, 2015; Liu et al., 2017; Lukito et al., 2020; Nickl-Jockschat et al., 2012; Via et al., 2011). These important findings notwithstanding, the intrinsic mechanisms and network topological organization that underpin the distribution of gray matter (GM) abnormalities in ASD remains largely unappreciated.

In recent years, advances in graph-theoretical analysis have begun to provide a conceptual framework for studying the topological properties of complex brain systems, which has led to the new field of connectomics. This line of research has been aiming to comprehensively map large-scale brain networks as a collection of nodes (brain regions or sub-areas) and edges (neural pathways or statistical relationships) (Sporns, 2013). The conceptual and empirical development of connectomics presents novel opportunities for understanding neuropsychiatric conditions, which now tend to be conceived of as brain networks disorders (Deco and Kringelbach, 2014; Fornito et al., 2017; Rubinov and Bullmore, 2013; van den Heuvel and Sporns, 2019). Moreover, there is an emerging consensus that the investigation of neuropathological patterns is ever more essential to improve diagnosis and prediction of mental illness (Cao et al., 2015; Huys et al., 2016; Yahata et al., 2017). This view is particularly relevant for psychiatric disorders. The U.S. National Institute of Mental Health's Research Domain Criteria (RDoC) takes into account network-level abnormalities as a core feature for understanding the neurobiology of mental disorders, with the aim to integrate the current symptom-based diagnostic classifications (Insel et al., 2010; Insel, 2014).

Despite advances in neuroimaging, graphs of GM alterations are particularly difficult to investigate. So far only a few studies have explored differences in GM systems in ASD using source-based morphometry (SoBM) (Grecucci et al., 2016; Pappaianni et al., 2018) and anatomical covariance, an MRI measure of cortical thickness or density relationships between brain areas (Evans, 2013). Although the neurobiological basis of anatomical covariance is still poorly understood (Alexander-Bloch et al., 2013), research on this topic has produced important findings in characterizing abnormal brain structures in ASD that appear to be part of the salience and default mode (Valk et al., 2015; Zheng et al., 2020; Zielinski et al., 2012), fronto-temporal (Bernhardt et al., 2014; Sharda et al., 2017), striatal (Eisenberg et al., 2015), parieto-occipital and limbic (Balardin et al., 2015; Bethlehem et al., 2017; Cardon et al., 2017) networks. A network neuroscience approach can better assess the anatomical alterations of ASD, reporting not only the sites of the alterations but also their mutual relationships.

An innovative computational methodology has been devised recently to perform *morphometric co-alteration networking* (MCN) analysis of human brain pathology, which can be defined as the investigation of abnormal conjoint patterns formed by localized GM co-altered regions (Cauda et al., 2018a). This type of analysis is a *meta*-connectomic and data-driven method, able to extend the information available from voxel-wise data. MCN can statistically derive the pathological network of a given brain disease using Patel's κ, an empirical Bayesian technique suitable for detecting the probability that alterations of two brain regions can co-occur (Patel et al., 2006; Smith et al., 2011). Different from the anatomical covariance method, MCN can identify a network in which the pathological modifications of GM are statistically related. It is therefore possible to examine the topological properties of GM co-alterations rather than those related to within-group anatomical covariance (Cauda et al., 2018a).

This innovative approach is well-suited to the study of pathophysiological alterations of brain disorders, which tend to be distributed across the brain according to network-like patterns (Fornito and Bullmore, 2015; Iturria-Medina and Evans, 2015; Raj et al., 2012; Stam, 2014). It has been proposed that mutual relationships of morphometric variation between two or more structurally defined regions reflects their shared vulnerability to damage due to processes of neuronal degeneration or neurodevelopmental factors (e.g., atypical dendritic growth, cellular migration, myelination, synaptogenesis and axonal pathfinding), and is mediated by molecular/cellular trophic and genetic effects (for a review see Fornito et al., 2015; Raj and Powell, 2018). Evidence for such mutual alteration distributions in autism exists (Casanova, 2006; Cauda et al., 2014; Galvez-Contreras et al., 2017; Nickl-Jockschat and Michel, 2011; Palmen et al., 2004; Wegiel et al., 2014; Zielinski et al., 2012); however, these distributions have not yet been comprehensively understood both from a micro- and macro-level perspective. Therefore, the identification of statistically robust and anatomically plausible co-alteration networks by means of the MCN methodology has the potential to reveal more about ASD pathophysiology than a canonical GM approach, since it better assesses the complex nature of morphometric abnormalities underlying the clinical hallmarks of disease.

Moreover, an emerging literature suggests that certain brain regions are preferentially vulnerable to a wide range of psychiatric and neurological disorders (Cauda et al., 2019b; Crossley et al., 2014; Goodkind et al., 2015; Liloia et al., 2018; Uddin, 2015). Typically, these regions are highly connected and play a pivotal role in supporting the integrity of brain network architecture (Buckholtz and Meyer-Lindenberg, 2012; Bullmore and Sporns, 2012; Crossley et al., 2014). In relation to their high topological centrality, these regions are to be conceived as pathological hubs capable of influencing the distribution of alterations within the cerebral parenchyma (Manuello et al., 2018; van den Heuvel and Sporns, 2013; Worbe, 2015; Zhou et al., 2012).

To date, the MCN methodology has been applied to find evidence of abnormal conjoint patterns in transdiagnostic *meta*-analyses (Cauda et al., 2020, 2018a, 2018b; Mancuso et al., 2020; Nani et al., 2021) and in studies on single neurological conditions such as Alzheimer's disease (Manuello et al., 2018) and chronic pain (Tatu et al., 2018). However, the presented approach has never been used to analyze data from individuals with ASD or other psychiatric conditions. Following the hypothesis that dysfunction at the systems' level characterizes this neurodevelopmental disorder (Ecker et al., 2013; Geschwind and Levitt, 2007), here we aim to provide a unique and comprehensive description of network topology of regional GM co-alterations in individuals with ASD. To further clarify the neurobiological basis of co-alterations, we also investigate the possible correspondence of MCN with normative structural and genetic co-expression connectivity. This choice is motivated by recent experimental proposals suggesting that the development of pathological alteration patterns are influenced by brain connectivity constraints (Cauda et al., 2020, 2018b; Shafiei et al., 2020), as well as by degeneration processes and maladaptive mechanisms (Fornito et al., 2015; Zhou et al., 2012). Finally, since we believe that the application of network science tools offer a powerful way of better understanding how pathology affects the brain (Filippi et al., 2013; Fornito and Bullmore, 2015; Fornito et al., 2017), this study takes advantage of graph-theoretical measures of centrality and clustering in order to provide new insights into large-scale GM co-alteration patterns in ASD.

2. Materials and methods

2.1. Data sources and search strategy

Meta-data of interest were identified in BrainMap (Fox et al., 2005; Laird et al., 2005b) and MEDLINE databases. First, the VBM BrainMap sector (Vanasse et al., 2018) was queried employing the software package Sleuth (v.3.0.3). The search logic was composed as follows:

- *[Experiments Contrast is Gray Matter] AND [Experiments Context is Disease Effects] AND [Subjects Diagnosis is Autism Spectrum Disorder] AND [Experiments Observed Changes is Controls > Patients]*;

A further systematic search was also carried out on the PubMed search engine (https://www.ncbi.nlm.nih.gov/pubmed/). Keywords terms were used as follows:

- *("Autism spectrum disorder" [title/abstract] OR "ASD" [title/abstract] OR "Autism" [title/abstract]) AND ("voxel-based morphometry" [title/abstract] OR "VBM" [title/abstract]).*

The search protocol adheres to the PRISMA Statement international guidelines (Liberati et al., 2009; Moher et al., 2009). This study is also compliant with the consensus-based rules for neuroimaging CBMA in psychiatric disorders (Muller et al., 2018; Tahmasian et al., 2019).

Up until December 2019, 118 full-text articles were reviewed systematically. We included experiments published in a peer-review journal a) using a whole-brain VBM analysis; b) reporting GM variations (i.e., decreased morphometric values) in subjects with ASD; c) adopting a between-group comparison with healthy controls; d) including stereotactic results in Talairach (TAL) or Montreal Neurological Institute (MNI) space.

We removed all the experimental groups having a sample size

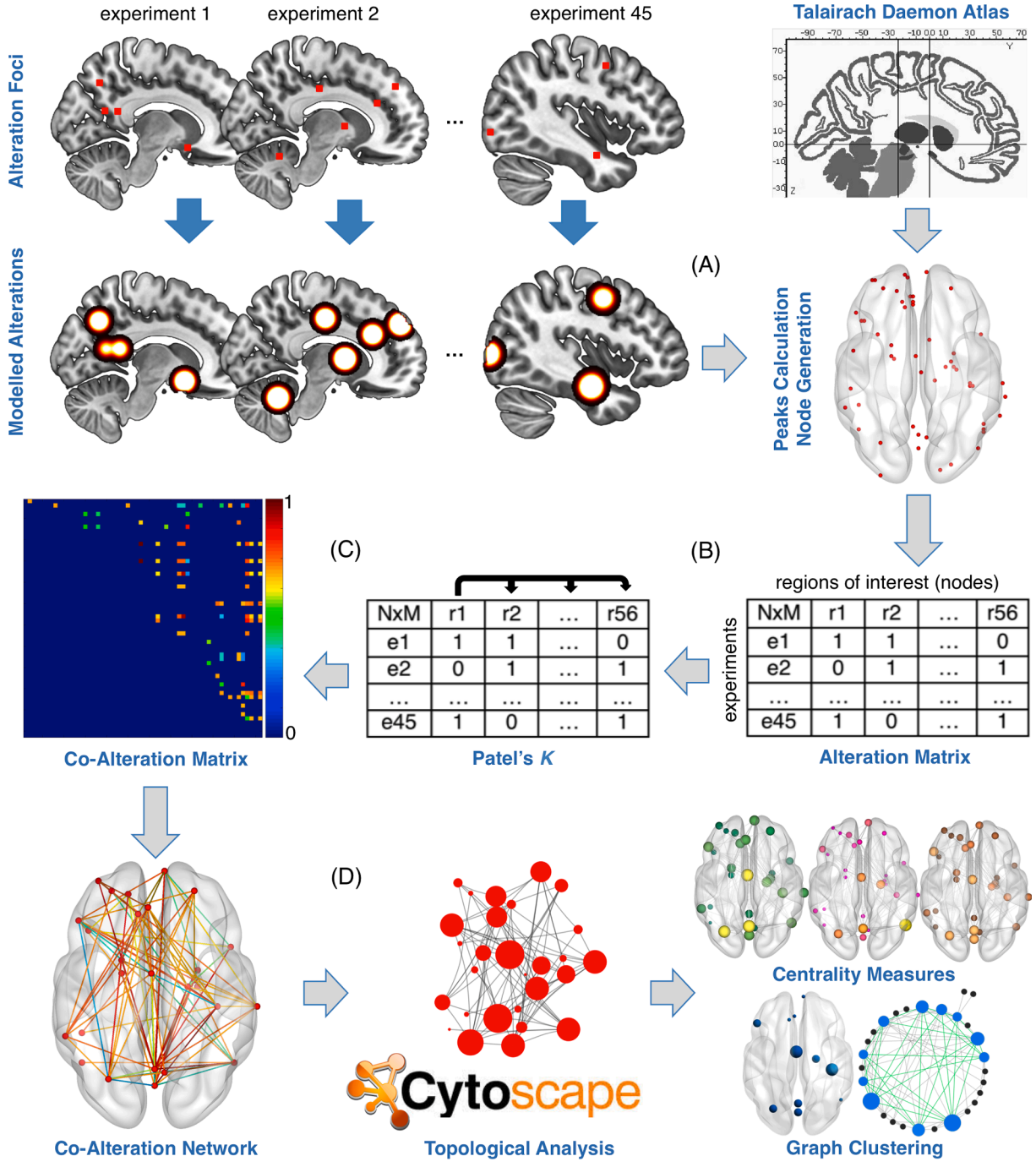

Fig. 1. Pipeline workflow of the method. (A) Meta-analytic estimation: For each VBM experiment included, the anatomical likelihood estimation (ALE) algorithm generated a modeled alteration (MA) map as the union of the 3-D Gaussian probability distribution of each alteration focus. (B) Alteration matrix creation: The general ALE map was created from the union of the MA maps and was fed to a peak detection algorithm to generate regions of interest (nodes). For each VBM experiment, nodes were considered altered if at least the 20% of their volume overlap with a MA map included. Thus, a binary vector was generated, able to describe if each node is altered/unaltered in each experiment. (C) Network detection: Using the Patel's κ index, the network of co-alteration probability was obtained. Specifically, the co-alteration strength was calculated between each one of such vectors and all the others. (D) Topological analysis: Using the resulting co-alteration matrix, graph-theoretical measures of centrality and clustering were computed.

smaller than 10 participants as previous recommended (Muller et al., 2018; Norman et al., 2016; Tahmasian et al., 2019). We also excluded experiments based on region-of-interest (ROI) analysis that did not analyze the whole brain (Muller et al., 2018). Additionally, to avoid the possibility of analyzing the same participants several times in a single study, we selected only the alteration foci reported by the largest experiment or the ones divided into diagnostic subcategories (for further details see also Table S1 – Checklist for neuroimaging CBMA).

2.2. Morphometric co-alteration network identification

2.2.1. Node definition

The anatomical likelihood estimation (ALE) results were used as priors for the *meta*-connectomic analysis. ALE is the most employed CBMA technique (Tahmasian et al., 2019); it can identify the spatial concordance of the morphological brain alterations between different neuroimaging experiments (Eickhoff et al., 2012, 2009). For each included experiment, the ALE algorithm generated a modeled alteration (MA) map as the union of the 3-D Gaussian probability distribution of each stereotactic coordinate (Fig. 1A). The final ALE map was obtained from the union of the MA maps.

To produce the MCN set of nodes, we individuated the local maxima of the ALE maps using a peak detection algorithm. Only the local maxima exhibiting the highest values survived this stage (i.e., values greater than the 90 percentile of the unthresholded ALE distribution). This step was crucial to consider only the altered loci with a very high consensus among the selected experiments. Thus, we reduced the number of nodes by adding a minimum spatial distance of 10 mm and a spherical ROI with a diameter of 10 mm was superimposed on the resulting peaks. The aforementioned threshold values employed are based on the quantitative estimates of the spatial uncertainty associated with the stereotactic coordinate in CBMA provided by Eickhoff et al. (2009), who evidenced an uncertainty in a spatial location with a mean of 10.2 mm (StDev = 0.4 mm). Therefore, the rationale behind this step is to minimize the redundancy of the co-alterations relating to the same cluster of variation that could potentially affect our subsequent topological analysis (Manuello et al., 2018). The Talairach Daemon (Lancaster et al., 2000) was finally used to label the anatomical areas.

To determine whether these nodes were altered in a given experiment, an MA map was produced for each experiment (Laird et al., 2005a). A 3-D Gaussian distribution of probability was built around each reported coordinate of a given experiment, for which standard deviation is smaller for a larger number of subjects, as proposed by Eickhoff et al. (2009). Then, MA was thresholded at $p = 0.01$ and overlaid on the set of nodes. Each node was considered to be altered for that experiment if at least 20% of its volume overlapped with a significant MA voxel. This step was crucial to avoid the detection of a false positive, given the possibility of considering a node as altered if it only includes the periphery of a distribution probability (Mancuso et al., 2019). For an in-depth and comprehensive discussion of the methodological steps, see also Manuello et al. (2018).

2.2.2. Co-alteration probability quantification

The set of nodes was used to build the MCN in ASD. We generated an alteration matrix $N \times M$, where each column corresponds to a node and each row represents an included experiment (Fig. 1B). By means of a Bernoulli generation data model, we determined the probability distribution of joint values of alteration for each pair of nodes. For each couple of nodes (a and b) it is possible to describe their state of co-occurrence with two binary variables representing four cases: both a and b altered; a altered and b non-altered; a non-altered and b altered; 4) both a and b non-altered:

$$\theta_1 = P(a = 1, b = 1)$$

$$\theta_2 = P(a = 1, b = 0)$$

$$\theta_3 = P(a = 0, b = 1)$$

$$\theta_4 = P(a = 0, b = 0)$$

Starting from the marginal probabilities, we calculated the co-alteration probability strength between each pair of nodes using the Patel's κ index (Patel et al., 2006; Smith et al., 2011) as:

$$\kappa = \frac{(\theta_1 - E)}{D(\max(\theta_1) - E) + (1 - D)(E - \min(\theta_1))}$$

where

$$E = (\theta_1 + \theta_2)(\theta_1 + \theta_3)$$

$$D = \begin{cases} \dfrac{\vartheta_1 - E}{2(max(\vartheta_1) - E)} + 0.5, if\, \vartheta_1 \geq E \\ 0.5 - \dfrac{\vartheta_1 - E}{2(E - min(\vartheta_1))}, otherwise \end{cases}$$

$$\min(\theta_1) = \max(0.2\theta_1 + \theta_2 + \theta_3 - 1)$$

$$\max(\theta_1) = \min(\theta_1 + \theta_2, \theta_1 + \theta_1 + \theta_3)$$

The numerator of the fraction calculates the difference between the probability that a and b occur to be co-altered and the expected probability E that a and b occur to be co-altered independently. E is the prior information of this Bayesian equation, which, in a frequentist framework, would be disregarded or treated as not fixed by the data. The denominator calculates a weighted normalizing constant so as to have the κ ranging from –1 and 1: an index that is close to 1 denotes high co-alteration (i.e., co-occurrence) between the nodes (Fig. 1C). The statistical significance of κ is assessed by means of a Monte Carlo simulation algorithm, a multinomial and generative model, which determines an estimate of $p(\kappa|z)$ by sampling a Dirichlet distribution and by calculating the proportion of the samples in which $\kappa > e$, where e is the threshold of statistical significance set to 0.01 (1,000 permutation runs). The obtained co-alteration matrix reports values proportional to the statistical occurrence between the alterations of the brain areas taken into account (Cauda et al., 2018a).

2.3. Topological analysis

Nodes and edges are the basic units of every network, and their accurate definition is of fundamental importance for a valid model of a complex system (Butts, 2009). Here, a large-scale brain analysis was employed: every node was defined as a peak of GM alteration, while the undirected binary edges represented the values of the thresholded Patel's κ. To determine the topological properties of the MCN in ASD, the corresponding co-alteration matrix was analyzed with Cytoscape (v.3.7.2.) (https://cytoscape.org/). Cytoscape is a bioinformatics software platform, which allows the analysis, modeling and visualization of biological networks and complex systems (Su et al., 2014). Then, the software application CentiScaPe (v.2.2) (Scardoni et al., 2014) was used to examine the topological properties of the nodes (Fig. 1D).

2.3.1. Measures of centrality

For each node of alteration, degree, closeness, and betweenness were determined in order to quantify the relevance of the node in the context of the MCN. These measures are cardinal indices of topological centrality (Freeman, 1978) and have been used collectively to examine the central network position of brain areas in both structural and functional connectomes (for a review see van den Heuvel and Sporns, 2013). Among them, degree centrality (D_C) is the simplest measure, which is formally defined as:

$$C_D(i) = k_i = \sum_{i \neq j} A_{ij}$$

In the formula, A_{ij} is a matrix of adjacency. The D_C is defined as the number of undirected links that are incident to a node, assuming that nodes with high connections exert more influence over network structure and function.

The closeness index can be conceived as the average tendency to node proximity or isolation. The closeness is calculated by determining the shortest path between the given node and all the others in the graph. The reciprocal of the summa is then calculated. Closeness centrality (C_C) is formally defined as the inverse of the average shortest path length:

$$C_C(i) = \frac{N-1}{\sum_{i \neq j} l_{ij}}$$

In the formula, l_{ij} is the shortest path length between nodes*i* and *j*. Of note, distance is related to the topological proximity. The C_C reflects the integration capacity of a node, as it can be conceived as the probability of the node to be relevant for several other nodes.

The betweenness index is determined by considering a pair of nodes (i, j) and counting the number of shortest paths connecting i and j that pass through another node (h). Betweenness centrality (B_C) measures the proportion of shortest paths between all pairs of nodes in the network that pass through a given node. Therefore, the B_C of a node i can be formally defined as:

$$C_B(i) = \frac{1}{(N-1)(N-2)} \sum_{h \neq i, h \neq j, j \neq i} l_{ij} \frac{p_{hj}(i)}{p_{hj}}$$

In the formula, $p_{hj}(i)$ indicates the number of shortest paths between h and j going through i, p_{hj} indicates the number of shortest paths between h and j, and $(N-1)(N-2)$ indicates the number of couples of nodes that do not include node i. The normalization by p_{hj} accounts for the possibility that several shortest paths may exist between any couple of nodes. Of note, the B_C value is associated with the total number of shortest paths connecting i and j. However, though a node can be crossed by only one path connecting i and j, if this path is the only one to link i and j, the node will have a high betweenness value. This implies that the node is essential in order to maintain the network connections.

Degree, closeness and betweenness are all measures of node prominence because they indicate which focal points, or brain areas in our case, occupy a central position in the network (i.e., *hubness* profile). Conceptually, these measures exhibit a considerable overlap in both real and simulated networks (Bolland, 1988); however, paying attention to different process by which key nodes might influence the distribution of the network. In particular, degree and closeness tend to be highly intercorrelated because they are directed centrality measures between nodes. By contrast, betweenness remains relatively uncorrelated with the degree and closeness, as it is an inherently asymmetric metric, measuring the frequency with which a node lies along paths that link other nodes (Valente et al., 2008).

Therefore, we defined node centrality on the grounds of different topological properties, aggregating rankings across all the measures to devise a more robust classification (Fornito et al., 2016). Specifically, we considered regions as pathological hubs when they reported the highest level of centrality (i.e., one standard deviation above the mean) across all three metrics (Fornito et al., 2016; van den Heuvel and Sporns, 2013).

2.3.2. Graph clustering

To provide a more specific characterization of the core architecture of the MCN, a network clustering analysis was performed. We applied the k-core decomposition algorithm as implemented in the Brain Connectivity Toolbox (Hagmann et al., 2008; Rubinov and Sporns, 2010), to reveal the hierarchical nucleus organization of the graph by gradually focusing on their central cores. This decomposition consists in identifying specific subsets of the graph (i.e., k-cores), each obtained by recursively eliminating all the nodes with a degree smaller than k, until the degree of all the surviving nodes is higher than or equal to k. Higher values of coreness indicate the nodes having greater degree and a more central position in the network's organization.

2.4. Correlation with brain connectivity profiles

To determine a possible correspondence of the MCN with normative patterns of brain connectivity, the Mantel's test – MT (Mantel, 1967) was applied. Specifically, we tested the relationship of similarity (i.e., Pearson's r) of the ASD co-alteration matrix with the structural and genetic co-expression connectivity matrices, respectively. The MT is a statistical test able to detect the correlation between two distance matrices. By means of a permutation test (i.e., Monte Carlo simulation), the significance of similarity was assessed. This step was crucial to overcome the problem of non-independence of elements in a distance matrix (Mantel, 1967). In this investigation we evaluated the statistical significance of any apparent departure from a zero correlation. To do so, each column and row of one of the two analyzed matrices was randomly permuted 5,000 times. The correlation was recalculated after each permutation, with a statistical significance consisting in the proportion of the permutations leading to a higher correlation coefficient. P-value was estimated after 5,000 permutations.

Analyses of the relationship of similarity between matrices were conducted in MNI space. Thus, we renormalized TAL coordinates of the co-altered nodes using the 'icbm2tal' algorithm developed by Lancaster et al. (2007).

2.4.1. Structural connectivity matrix

The structural connectivity matrix was generated from the diffusion tensor imaging (DTI) data set provided by the WU-Minn Human Connectome Project (900 Subjects data release, 2015 Q4) (Van Essen et al., 2013). DTI data were acquired from 842 healthy subjects using a multishell diffusion scheme (diffusion sampling directions: 90, 90, 90; in-plane resolution and slice thickness: 1.25 mm; b-values: 1000, 2000, 3000 s/mm^2). The spatial normalization of the DTI data was conducted by the q-space diffeomorphic reconstruction method (Yeh and Tseng, 2011), which can obtain the spin distribution function in the MNI stereotactic space (resolution: 1 mm; sampling length ratio: 1.25). Averaging the spike density functions of all subjects, an atlas was created. Thus, the generalized q-sampling imaging (GQI) method (Yeh et al., 2010) was employed to detect the structural pathways. In this investigation the GQI was able to obtain 5,000 seeds in the whole-brain. Only the seeds corresponding to our co-altered nodes, obtained previously with the MCN approach, were employed to calculate the structural matrix by using the numbers of fiber tracts passing between two seeds normalized by the median length of the connecting paths.

2.4.2. Genetic co-expression connectivity matrix

The genetic co-expression connectivity matrix was generated from the microarray data sets provided by the Allen Human Brain Atlas (AHBA) Project (Hawrylycz et al., 2012). Complete normalized microarray data were acquired from six healthy human brains. The AHBA data set was processed using the workflow pipeline for relating brain-wide gene expression profile to neuroimaging results developed by Arnatkeviciute et al. (2019a). The processing steps were performed as implemented in the code available at github (https://github.com/BMHLab/AHBAprocessing) (for an in-depth discussion of the methodological steps, see also Arnatkeviciute et al., 2019a). To note, the differential stability measure (Hawrylycz et al., 2015) of gene filtering was used to derive gene patterns expressed consistently across all AHBA brains. Also, the 1,000 seeds parcellation (Schaefer et al., 2018) was applied to identify regions spatially corresponding to the MCN nodes. Only the seeds corresponding to our nodes were employed to generate the gene expression × node matrix.

2.5. Distribution of the nodes across canonical networks and network-betweenness estimation

To evaluate the impact of GM alterations on different functional large-scale networks, each co-altered node was assigned in data-driven manner to one of the 7 networks of the parcellation proposed by Yeo et al. (2011), who parceled the human cerebral cortex using resting-state fMRI data from 1000 healthy volunteers. Nodes falling in the basal nuclei and cerebellum were assigned to one of Yeo's networks using the striatal (Choi et al., 2012) and cerebellar (Buckner et al., 2011) parcellations, respectively. We tested if the spatial distribution of the alteration nodes across canonical networks was different from chance by creating 28 random GM nodes (corresponding to the number of the co-altered nodes of our network, see below), and repeating the procedure 1000 times. The significance of the numerosity of each network's nodes was tested against the resulting null distributions.

For each network, its network-betweenness – NB (Cauda et al., 2020; Mancuso et al., 2020) was estimated as the ratio between the number of co-alteration edges connecting its nodes to the nodes belonging to other networks and the total number of edges incident upon its nodes. To test whether the NB of each network was significantly different from chance, the co-alteration network was randomized 1000 times using a Maslov-

Table 1
Brain areas (nodes) of the gray matter morphometric co-alteration network. Node labeling, morphometric location (Talairach Daemon Labels) and Talairach coordinates were expressed for both co-altered and non co-altered nodes.

Node ID	Node label	Anatomical region (Brodmann area)	Hemisphere	Talairach			Co-altered
				x	y	z	
1	**Crus2_L**	**Crus II (cerebellum)**	**Left**	**−44**	**−58**	**−44**	**Yes**
2	**Crus2_R**	**Crus II (cerebellum)**	**Right**	**48**	**−58**	**−44**	**Yes**
3	ML9	Medial lobule IX (cerebellum)	Left	−4	−56	−42	No
4	**FG**	**Fusiform gyrus (BA 37)**	**Right**	**26**	**−2**	**−38**	**Yes**
5	Crus1	Crus I (cerebellum)	Right	48	−54	−32	No
6	**Crus1**	**Crus I (cerebellum)**	**Left**	**−44**	**−40**	**−32**	**Yes**
7	**BA38**	**Temporopolar cortex (BA 38)**	**Right**	**46**	**12**	**−30**	**Yes**
8	**BA28**	**Parahippocampal gyrus (BA 28)**	**Right**	**26**	**−12**	**−28**	**Yes**
9	Unc	Uncus (BA 20)	Right	28	−14	−26	No
10	Dec	Declive (cerebellum)	Right	24	−84	−22	No
11	**Amy_R**	**Amygdala**	**Right**	**24**	**−8**	**−22**	**Yes**
12	OG	Orbital gyrus (BA 11)	Left	−4	40	−22	No
13	IFG	Inferior frontal gyrus (BA 11)	Left	−12	36	−20	No
14	RG	Rectal gyrus (BA 11)	Left	−6	40	−20	No
15	**PHG**	**Parahippocampal gyrus (BA 34)**	**Right**	**20**	**−12**	**−14**	**Yes**
16	Hip	Hippocampus	Left	−18	−6	−14	No
17	BA10	Superior frontal gyrus (BA 10)	Left	−10	56	−12	No
18	**OFG_R**	**Orbitofrontal gyrus (BA 10)**	**Right**	**6**	**58**	**−12**	**Yes**
19	BA37	Fusiform gyrus (BA 37)	Right	48	−60	−10	No
20	MTG	Middle temporal gyrus (BA 37)	Right	60	−48	−10	No
21	**Amy_L**	**Amygdala**	**Left**	**−20**	**−4**	**−10**	**Yes**
22	BA47	Inferior frontal gyrus (BA 47)	Left	−30	12	−10	No
23	MFG_R	Medial frontal gyrus (BA 10)	Right	6	58	−10	No
24	BA17	Inferior occipital gyrus (BA 17)	Right	16	−88	−8	No
25	**Pu**	**Putamen**	**Left**	**−20**	**4**	**−8**	**Yes**
26	OFG_L	Middle orbital gyrus (BA 10)	Left	−32	52	−8	No
27	IOG	Inferior occipital gyrus (BA 18)	Right	44	−72	−6	No
28	**Cd**	**Caudate tail**	**Right**	**38**	**−24**	**−6**	**Yes**
29	**BA11**	**Middle frontal gyrus (BA 11)**	**Left**	**−34**	**52**	**−6**	**Yes**
30	Cl	Claustrum	Right	38	−26	−4	No
31	AI_R	Anterior insula (BA 13)	Right	40	−26	−4	No
32	**STG**	**Superior temporal gyrus (BA 22)**	**Right**	**62**	**−24**	**−2**	**Yes**
33	ACC_L	Anterior cingulate cortex (BA 10)	Left	−8	54	−2	No
34	**AI_L**	**Anterior insula (BA 13)**	**Left**	**−40**	**22**	**0**	**Yes**
35	BA22	Middle temporal gyrus (BA 22)	Right	64	−34	2	No
36	IFG_Tri	Inferior frontal gyrus (BA 47)	Left	−42	22	2	No
37	**IFG**	**Inferior frontal gyrus (BA 45)**	**Left**	**−46**	**28**	**2**	**Yes**
38	**LG**	**Lingual gyrus (BA 18)**	**Left**	**0**	**−72**	**8**	**Yes**
39	**PCC**	**Posterior cingulate cortex (BA 30)**	**Left**	**0**	**−62**	**10**	**Yes**
40	Pulv	Pulvinar (thalamus)	Right	12	−22	10	No
41	MDN	Medial dorsal nucleus (thalamus)	Right	2	−16	10	No
42	**MFG_L**	**Middle frontal gyrus (BA 10)**	**Left**	**−26**	**46**	**10**	**Yes**
43	BA18	Middle occipital gyrus (BA 18)	Left	−28	−92	12	No
44	**BA9**	**Medial frontal gyrus (BA 9)**	**Left**	**−16**	**44**	**20**	**Yes**
45	IPL	Inferior parietal lobule (BA 40)	Left	−50	−28	22	No
46	**SM**	**Supramarginal gyrus (BA 40)**	**Left**	**−54**	**−42**	**24**	**Yes**
47	**vACC**	**Ventral anterior cingulate (BA 24)**	**Left**	**−2**	**−4**	**26**	**Yes**
48	PCG	Precentral gyrus (BA 6)	Left	−48	0	28	No
49	**PCUN_R**	**Precuneus (BA 7)**	**Right**	**6**	**−64**	**36**	**Yes**
50	BA6	Medial frontal gyrus (BA 6)	Left	−4	34	36	No
51	**SFG_R**	**Superior frontal gyrus (BA 9)**	**Right**	**24**	**46**	**36**	**Yes**
52	**MOG**	**Middle occipital gyrus (BA 19)**	**Left**	**−28**	**−68**	**38**	**Yes**
53	**PCUN_L**	**Precuneus (BA 7)**	**Left**	**0**	**−62**	**38**	**Yes**
54	**BA8**	**Superior medial frontal gyrus (BA 8)**	**Left**	**−10**	**32**	**38**	**Yes**
55	ACC_R	Anterior cingulate cortex (BA 32)	Right	8	8	40	No
56	**SFG_L**	**Superior frontal gyrus (BA 9)**	**Left**	**−4**	**36**	**42**	**Yes**

Bold text = Co-altered nodes; No bold = Non-altered nodes.

Sneppen algorithm (Maslov and Sneppen, 2002; Rubinov and Sporns, 2010); the NB of each network was recalculated in each iteration to obtain 7 NB distributions. A one-sample two-tailed *t*-test was used to assess the significance of the 7 NBs (Cauda et al., 2020).

3. Results

We included 42 published articles. Specifically, we analyzed *meta*-data coming from 45 VBM experiments, including 3,576 subjects (1,786 with diagnosis of ASD and 1790 healthy controls) and 244 coordinates of GM variation. The analysis was carried out in the TAL space. Original MNI coordinates were converted using the 'icbm2tal' algorithm (Lancaster et al., 2007) in order to correct the spatial disparity between coordinate (x-y-z) results (Laird et al., 2010), thus promoting accuracy of the *meta*-analytic synthesis (Muller et al., 2018; Tahmasian et al., 2019). For the systematic study selection see Fig. S1 and Table S1. For detailed information about the clinical and methodological characteristics of the selected *meta*-data, see also Tables S2 and S3, respectively.

3.1. General characterization of co-alterations

Our *meta*-connectomic and data-driven approach reveals that it is possible to identify a quantifiable co-alteration network of GM abnormalities in ASD. On the grounds of the ALE *meta*-data, our ROI generation procedure derived 56 nodes (see also Table 1 and Table S4 for the morphometric location of nodes and their coordinates in TAL and MNI space, respectively). However, only 28 nodes exhibit statistically significant edges of co-alteration, encompassing cortical, basal nuclei and cerebellar regions. With regard to the anatomical distribution of the nodes, we observe that they can be found in both perceptual lower-level and multimodal regions and that some of them show a symmetric position across hemispheres. This is the case of the amygdala, precuneus and the cerebellar crus II.

Fig. 2 reports the whole co-alteration pattern showing 91 edges (45 interhemispheric and 46 intrahemispheric). Most of the edges involve fronto-cerebellar, limbic-striatal and fronto-parietal regions. A complex pattern of co-alteration was also detected for occipital and superior temporal nodes. Patel's κ values range from 0.79 of the right amygdala-parahippocampal-basal ganglia structures to the 0.23 of the edges of the middle occipital-inferior frontal regions. High κ values are also associated to the left precuneus (PCUN_L), lingual gyrus (LG_L) and posterior cingulate cortex (PCC_L), as well as to the right orbitofrontal gyrus (OFG_R), temporopolar pole (BA_38_R) and posterior cerebellar lobe (Crus2_R) (see Table 2 for the κ values graph).

3.2. Level of the centrality of nodes

Fig. 3 illustrates the level of topological position of the nodes. The co-altered nodes are represented in different colors and sizes according to their values of degree, betweenness and closeness centrality. The PCUN_L and ventral anterior cingulate cortex (vACC_L) show the highest values of degree (12 edges), followed by the left middle occipital gyrus (MOG_L, 11 edges) and right Crus2, tail of caudate (Cd_R), left inferior frontal gyrus (IFG_L), LG_L and right parahippocampal area (PHG_R) (10 edges). By contrast, the left anterior insular and cerebellar regions (i.e., AI_L and Crus2_L) exhibit the lowest values of degree. Values of closeness range from 0.34 to 0.63, with the highest values associated with the PCUN_L, followed by the vACC_L, MOG_L, IFG_L, Cd_R and PHG_R. Also for this measure, the AI_L and Crus2_L show the lowest values. Relative to the betweenness, the Crus2_R reports the highest value, followed, in order, by the PCUN_L, PHG_R, vACC_L, MOG_L and OFG_R.

Next, we investigated in detail the pathological *hubness* profile of the regions. To do so, we identified the nodes reporting the highest level of centrality (i.e., one standard deviation above the mean) across all three metrics. The analysis reveals a central network position for the PCUN_L [TAL × = 0; y = -62; z = 38], vACC_L [TAL × = -2; y = -4; z = 26] and MOG_L [TAL × = -28; y = -68; z = 38]. For a graphical representation of results and node-specific values of degree, betweenness and closeness of each node of the MCN, see Fig. 4.

3.3. Core sub-graph

Since highly interconnected nodes characterize the MCN of ASD, we investigated the possibility of identifying the most central sub-graph and its hierarchical components. The implementation of the k-core decomposition algorithm allowed us to detect a core nucleus composed of 15 nodes and 57 edges using a k degree = 6, including frontal (i.e., OFG_R, left superior, medial and inferior frontal gyri), subcortical (vACC_L, PHG_R, Cd_R, left putamen and right amygdala), occipital (LG_L and MOG_L), temporo-parietal (PCUN_L, right superior temporal gyrus and left supramarginal gyrus) and cerebellar (Crus2_R) areas (Fig. 5).

3.4. Correlation with the brain connectivity profiles

The Mantel test employed to investigate whether or not GM co-alterations overlap the structural or genetic connectivity profiles showed that the ASD co-alterations are significantly correlated with the anatomical connectivity ($r = 0.14$, $p < 0.027$). Finally, the comparison with the genetic co-expression connectivity matrix reports non-

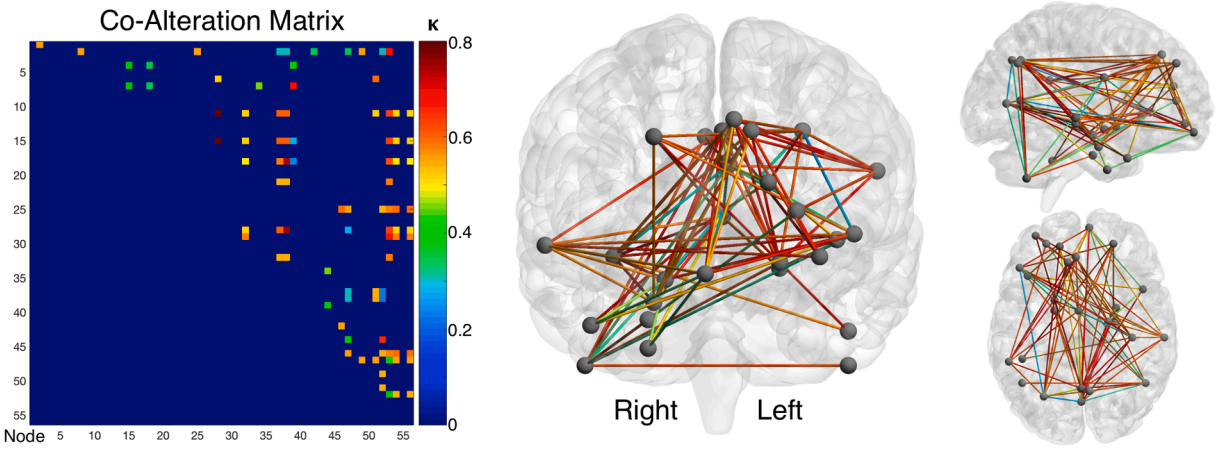

Fig. 2. The gray matter morphometric co-alteration network of autism spectrum disorder. Both co-alteration matrix and brain network related to gray matter abnormalities are shown. Edge colors from blue to red mean increasing Patel's κ values (i.e., increasing co-alteration probabilities). Unconnected nodes are not reported. The images were generated by the BrainNet application (Xia et al., 2013). (For interpretation of the references to colour in this figure legend, the reader is referred to the web version of this article.)

Table 2
Edge co-alteration strength between co-altered nodes (Patel's k). Node labeling, Talairach coordinates and Yeo's network classification were expressed for each co-altered node.

Node	Talairach			Yeo's Network	Patel's k	Node	Talairach			Yeo's Network
	x	y	z				x	y	z	
Amy_R	24	−8	−22	Limbic	0.790	Cd_R	38	−24	−6	FPN
PHG_R	20	−12	−14	Limbic	0.790	Cd_R	38	−24	−6	FPN
Cd_R	38	−24	−6	FPN	0.755	LG_L	0	−72	8	Visual
OFG_R	6	58	−12	DMN	0.742	LG_L	0	−72	8	Visual
BA_11_L	−34	52	−6	DMN	0.685	PCUN_L	0	−62	38	DMN
BA_38_R	46	12	−30	DMN	0.669	PCC_L	0	−62	10	DMN
Crus2_R	48	−58	−44	FPN	0.669	PCUN_L	0	−62	38	DMN
BA_9_L	−16	44	20	DMN	0.652	MOG_L	−28	−68	38	Visual
Amy_R	24	−8	−22	Limbic	0.634	PCUN_L	0	−62	38	DMN
PHG_R	20	−12	−14	Limbic	0.634	PCUN_L	0	−62	38	DMN
Cd_R	38	−24	−6	FPN	0.634	PCUN_L	0	−62	38	DMN
OFG_R	6	58	−12	DMN	0.615	PCUN_L	0	−62	38	DMN
Amy_R	24	−8	−22	Limbic	0.602	IFG_L	−46	28	2	FPN
PHG_R	20	−12	−14	Limbic	0.602	IFG_L	−46	28	2	FPN
Cd_R	38	−24	−6	FPN	0.602	IFG_L	−46	28	2	FPN
Amy_R	24	−8	−22	Limbic	0.602	LG_L	0	−72	8	Visual
PHG_R	20	−12	−14	Limbic	0.602	LG_L	0	−72	8	Visual
Pu_L	−20	4	−8	SN/VAN	0.600	SM_L	−54	−42	24	SN/VAN
Crus1_L	−44	−40	−32	SN/VAN	0.600	SFG_R	24	46	36	FPN
Pu_L	−20	4	−8	SN/VAN	0.600	BA_8_L	−10	32	38	FPN
SM_L	−54	−42	24	SN/VAN	0.600	BA_8_L	−10	32	38	FPN
Pu_L	−20	4	−8	SN/VAN	0.600	SFG_L	−4	36	42	DMN
SM_L	−54	−42	24	SN/VAN	0.600	SFG_L	−4	36	42	DMN
OFG_R	6	58	−12	DMN	0.581	IFG_L	−46	28	2	FPN
BA_11_L	−34	52	−6	DMN	0.580	STG_R	62	−24	−2	SMN
Amy_L	−20	−4	−10	Limbic	0.580	PCUN_L	0	−62	38	DMN
Pu_L	−20	4	−8	SN/VAN	0.580	PCUN_L	0	−62	38	DMN
STG_R	62	−24	−2	SMN	0.580	PCUN_L	0	−62	38	DMN
SM_L	−54	−42	24	SN/VAN	0.580	PCUN_L	0	−62	38	DMN
BA_11_L	−34	52	−6	DMN	0.580	BA_8_L	−10	32	38	FPN
BA_11_L	−34	52	−6	DMN	0.580	SFG_L	−4	36	42	DMN
Crus2_L	−44	−58	−44	FPN	0.560	Crus2_R	48	−58	−44	DMN
Crus2_R	48	−58	−44	DMN	0.560	BA_28_R	26	−12	−28	Limbic
Crus2_R	48	−58	−44	DMN	0.560	Pu_L	−20	4	−8	SN/VAN
MFG_L	−26	46	10	DMN	0.560	SM_L	−54	−42	24	SN/VAN
Pu_L	−20	4	−8	SN/VAN	0.560	vACC_L	−2	−4	26	SN/VAN
SM_L	−54	−42	24	SN/VAN	0.560	vACC_L	−2	−4	26	SN/VAN
Crus2_R	48	−58	−44	DMN	0.560	PCUN_R	6	−64	36	DMN
vACC_L	−2	−4	26	SN/VAN	0.560	PCUN_R	6	−64	36	DMN
vACC_L	−2	−4	26	SN/VAN	0.560	SFG_R	24	46	36	FPN
vACC_L	−2	−4	26	SN/VAN	0.560	BA_8_L	−10	32	38	FPN
vACC_L	−2	−4	26	SN/VAN	0.560	SFG_L	−4	36	42	DMN
Amy_L	−20	−4	−10	Limbic	0.538	IFG_L	−46	28	2	FPN
STG_R	62	−24	−2	SMN	0.538	IFG_L	−46	28	2	FPN
Amy_L	−20	−4	−10	Limbic	0.538	LG_L	0	−72	8	Visual
STG_R	62	−24	−2	SMN	0.538	LG_L	0	−72	8	Visual
IFG_L	−46	28	2	FPN	0.538	SFG_R	24	46	36	FPN
LG_L	0	−72	8	Visual	0.538	SFG_R	24	46	36	FPN
Pu_L	−20	4	−8	SN/VAN	0.538	MOG_L	−28	−68	38	Visual
SM_L	−54	−42	24	SN/VAN	0.538	MOG_L	−28	−68	38	Visual
PCUN_R	6	−64	36	DMN	0.538	MOG_L	−28	−68	38	Visual
SFG_R	24	46	36	FPN	0.538	MOG_L	−28	−68	38	Visual
MOG_L	−28	−68	38	Visual	0.538	BA_8_L	−10	32	38	FPN
MOG_L	−28	−68	38	Visual	0.538	SFG_L	−4	36	42	DMN
Crus1_L	−44	−40	−32	SN/VAN	0.515	Cd_R	38	−24	−6	FPN
Amy_R	24	−8	−22	Limbic	0.515	STG_R	62	−24	−2	SMN
PHG_R	20	−12	−14	Limbic	0.515	STG_R	62	−24	−2	SMN
Cd_R	38	−24	−6	FPN	0.515	STG_R	62	−24	−2	SMN
Amy_R	24	−8	−22	Limbic	0.515	SFG_R	24	46	36	FPN
Amy_R	24	−8	−22	Limbic	0.515	BA_8_L	−10	32	38	FPN
PHG_R	20	−12	−14	Limbic	0.515	BA_8_L	−10	32	38	FPN
Cd_R	38	−24	−6	FPN	0.515	BA_8_L	−10	32	38	FPN
Amy_R	24	−8	−22	Limbic	0.515	SFG_L	−4	36	42	DMN
PHG_R	20	−12	−14	Limbic	0.515	SFG_L	−4	36	42	DMN
Cd_R	38	−24	−6	FPN	0.515	SFG_L	−4	36	42	DMN
OFG_R	6	58	−12	DMN	0.490	STG_R	62	−24	−2	SMN
OFG_R	6	58	−12	DMN	0.490	BA_8_L	−10	32	38	FPN
OFG_R	6	58	−12	DMN	0.490	SFG_L	−4	36	42	DMN
BA_38_R	46	12	−30	DMN	0.461	AI_L	−40	22	0	SN/VAN
AI_L	−40	22	0	SN/VAN	0.461	BA_9_L	−16	44	20	DMN
FFG_R	26	−2	−38	Limbic	0.435	PCC_L	0	−62	10	DMN
PCC_L	0	−62	10	DMN	0.435	BA_9_L	−16	44	20	DMN

(*continued on next page*)

Table 2 (*continued*)

Node	Talairach			Yeo's Network	Patel's k	Node	Talairach			Yeo's Network
	x	y	z				x	y	z	
BA_9_L	−16	44	20	DMN	0.435	vACC_L	−2	−4	26	SN/VAN
vACC_L	−2	−4	26	SN/VAN	0.435	PCUN_L	0	−62	38	DMN
MOG_L	−28	−68	38	Visual	0.408	PCUN_L	0	−62	38	DMN
FFG_R	26	−2	−38	Limbic	0.379	PHG_R	20	−12	−14	Limbic
BA_38_R	46	12	−30	DMN	0.379	PHG_R	20	−12	−14	Limbic
FFG_R	26	−2	−38	Limbic	0.348	OFG_R	6	58	−12	DMN
BA_38_R	46	12	−30	DMN	0.348	OFG_R	6	58	−12	DMN
Crus2_R	48	−58	−44	DMN	0.342	MFG_L	−26	46	10	DMN
Crus2_R	48	−58	−44	DMN	0.342	vACC_L	−2	−4	26	SN/VAN
Crus2_R	48	−58	−44	DMN	0.311	IFG_L	−46	28	2	FPN
Crus2_R	48	−58	−44	DMN	0.311	LG_L	0	−72	8	Visual
IFG_L	−46	28	2	FPN	0.311	vACC_L	−2	−4	26	SN/VAN
LG_L	0	−72	8	Visual	0.311	vACC_L	−2	−4	26	SN/VAN
Crus2_R	48	−58	−44	DMN	0.311	MOG_L	−28	−68	38	Visual
PHG_R	20	−12	−14	Limbic	0.277	PCC_L	0	−62	10	DMN
Cd_R	38	−24	−6	FPN	0.277	vACC_L	−2	−4	26	SN/VAN
OFG_R	6	58	−12	DMN	0.242	PCC_L	0	−62	10	DMN
IFG_L	−46	28	2	FPN	0.235	MOG_L	−28	−68	38	Visual
LG_L	0	−72	8	Visual	0.235	MOG_L	−28	−68	38	Visual

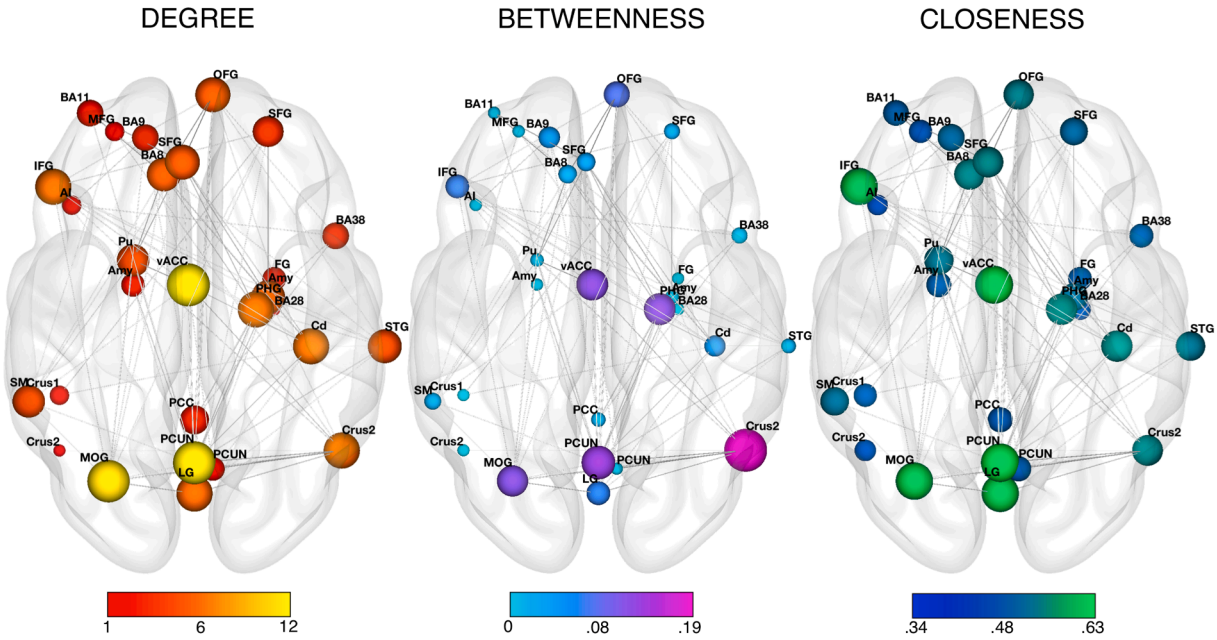

Fig. 3. Superposition of the topological analysis of the gray matter morphometric co-alteration network (MCN) on 3-D brain axial slices. Left template: Degree centrality values of the MCN in autism spectrum disorder. Central template: Betweenness centrality values of the MCN in autism spectrum disorder. Right template: Closeness centrality values of the MCN in autism spectrum disorder. The colors and dimensions of the nodes indicate their network centrality (bigger node: higher centrality; from red to yellow, from light blue to purple and from dark blue to green: from lower to higher values of degree, betweenness and closeness centrality, respectively). Slices are shown in neurological convention (i.e., right is right, left is left). (For interpretation of the references to colour in this figure legend, the reader is referred to the web version of this article.)

significant results at $p = 0.05$.

3.5. Distribution of the nodes across canonical networks and network-betweenness

The parcellation search revealed the presence of at least one node for six out of seven canonical networks, namely the default mode network (DMN), frontoparietal network (FPN), salience/ventral attentional network (SN/VAN), limbic network, visual network and the sensorimotor network (SMN). In particular, the DMN reports the highest number of co-altered nodes (10/28, 35.7% of the total) mainly located in fronto-parietal areas. The number of nodes of the DMN was greater than a random null model ($p = 0.06$). By contrast, the number of nodes related to the Limbic, SN/VAN FPN and Visual networks was not significantly different from chance. The SMN network showed only a single node located in the right STG (Fig. 6 left panel), while in the null model there were significantly more nodes ($p = 0.04$). The dorsal attentional network (DAN) had no co-altered nodes, which was significant when compared to the random extraction ($p = 0.02$). It is important to clarify that these results do not indicate that the functionally defined SMN and DAN regions are not altered in subjects with ASD, but rather that their alterations are not associated with that in other nodes.

With regard to the 91 edges, only 17 edges connect nodes of the same functional network, whereas 81.6% of them connect nodes belonging to different networks (Fig. 6 right panel). Table 3 indicates the NB of each one of the 7 networks identified by Yeo et al. (2011). With the exception of the DAN, which is not represented by any node of alteration, each one of the canonical networks have a very high NB, that is, the edges of co-

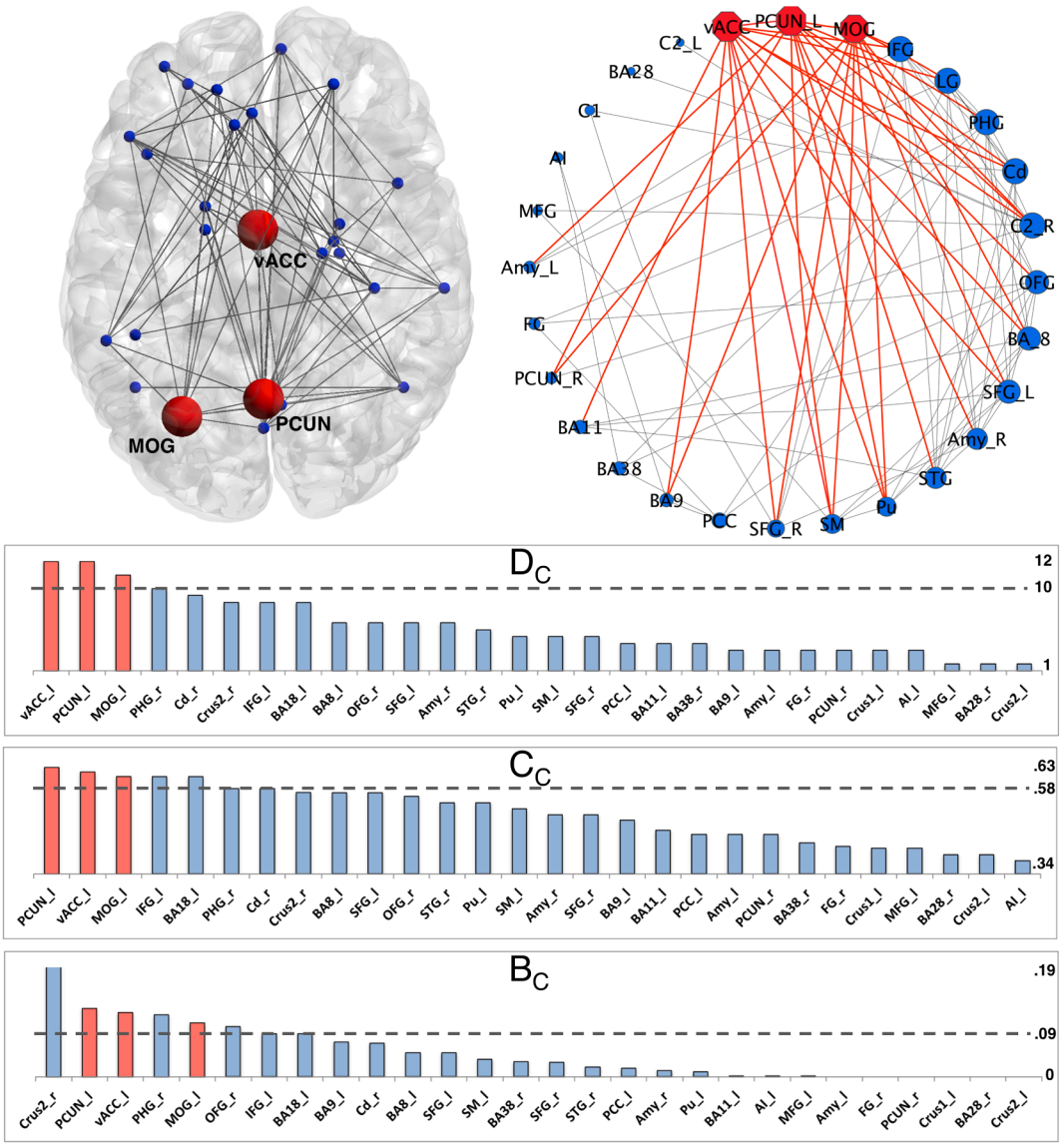

Fig. 4. Specific centrality values of degree (D_C), closeness (C_C) and betweenness (B_C) of each of the 28 co-altered nodes of the morphometric co-alteration network in ASD. The red nodes and bars mark the brain areas that report the highest level of centrality across all three metrics (i.e., > one standard deviation of the mean). The figure also illustrates the anatomical position of the brain pathological hubs and their co-alterations using the circular layout algorithm of Cytoscape software application (https://cytoscape.org/). (For interpretation of the references to colour in this figure legend, the reader is referred to the web version of this article.)

alteration often connect nodes that are placed in two different functional networks rather than in the same one. The DMN is the more co-altered with itself, while the nodes belonging to the SMN only connect with nodes of other networks. However, the Maslov-Sneppen null model (Cauda et al., 2020; Maslov and Sneppen, 2002) indicates that, given our starting nodes, only the DMN-NB is significantly higher than chance ($p < 0.001$). All the other networks' NB, SMN included, are not different from the null model. The apparent contradiction of having the DMN-NB as the lowest one of the 7 canonical networks, but also significantly higher than chance, is probably due to the fact that the DMN is the most represented network in terms nodes of alteration. Thus, the number of within-DMN co-alteration edges is obviously high (Fig. 6 bottom panel); however, given the node distribution across the networks, this is not a surprising result, as it could be expected to be even higher.

4. Discussion

To the best of our knowledge, this is the first *meta*-analytic study that mapped the unknown GM topology in individuals with ASD, using the canonical ALE framework as priors for an unbiased and connectome-wide analysis. Our findings provide evidence that neuroanatomical variations in ASD tend to form a complex network of co-alteration, encompassing multiple defined cortical, subcortical and cerebellar sites. Within this co-alteration network, certain higher-order areas (i.e., vACC, PCUN and MOG) exhibit a substantial hierarchical profile, and thereby they are conceivable as pathological hubs. Further, we reveal that the organization of co-alterations reflects a biologically plausible distribution, mirroring in part the constraints of brain structural connectivity. Altogether, these results extend previous literature reporting morphometric variations in the ASD pathophysiology, emphasizing the necessity of considering this spectrum of disorders as a network-like dysfunction of spatially distributed GM sites.

Significantly, our findings demonstrate that regional GM abnormalities are not independent in ASD. Instead, multiple neural subpopulations report a morphometric change that statistically co-occurs with an alteration in other brain sites. This result is consistent with recent neuroimaging literature suggesting a structural signature of brain architecture in other psychiatric disorders, such as schizophrenia

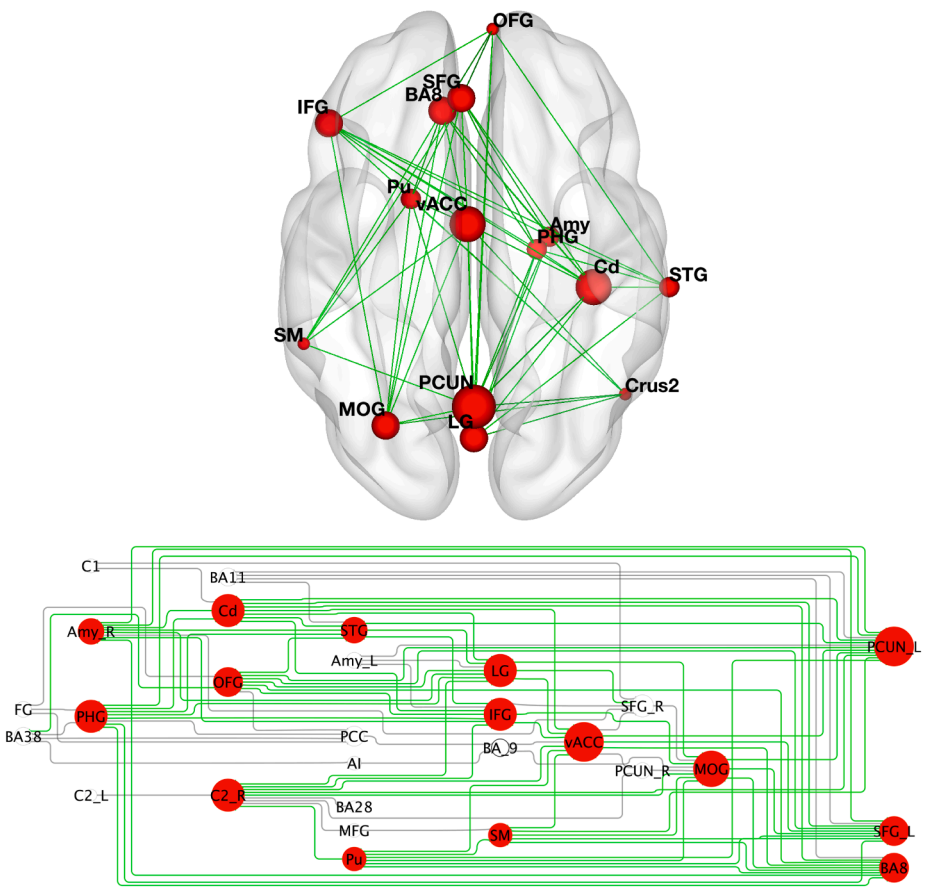

Fig. 5. Brain network clustering results using the k-core decomposition algorithm. Upper panel: Superposition of the k-core values of the morphometric co-alteration network on 3-D brain template. Bottom panel: Graphical illustration of the clustering values using the hierarchical layout algorithm of Cytoscape software application (https://cytoscape.org/). The colors and dimensions of the nodes indicate their network centrality (red node: brain areas with highest hierarchy; bigger node: higher degree centrality). (For interpretation of the references to colour in this figure legend, the reader is referred to the web version of this article.)

(Cauda et al., 2020; Shafiei et al., 2020; van den Heuvel et al., 2010), major depression (Korgaonkar et al., 2014; Zheng et al., 2019), obsessive-compulsive disorder (Cao et al., 2021; Reess et al., 2016) and bipolar disorder (Ajilore et al., 2015; Collin et al., 2016; Fernandes et al., 2019). Our analysis reveals robust co-alterations between a distinct set of regions that have been consistently reported to be altered and associated with clinical manifestations in previous MRI-based investigations in ASD. However, different from classical anatomical neuroimaging techniques such as VBM or cortical thickness, which do not assess any kind of topological relationship between regions (Ashburner and Friston, 2001), our graphical analysis was able to consider neuroanatomical abnormalities (nodes) and their statistical mutual relationship (edges) as a network unit (Cauda et al., 2018b). Therefore, our results can be understood in the context of a spatially distributed model rather than of isolated neural loci.

Anatomical abnormalities have been observed in different cerebral systems, encompassing a set of multimodal, cerebellar, perceptual and limbic nodes. This large-scale distribution and its conjoint patterns of alteration might be considered as a clinical implication of the phenotypic heterogeneity of ASD (Wylie et al., 2020) and might also derive from an abnormal neural development (Frith, 2004; Kim et al., 2017; Neniskyte and Gross, 2017; Thomas et al., 2016) or compensatory responses (Fornito et al., 2015; Zhou et al., 2012).

The present findings, along with recent proposals (Balardin et al., 2015; Ecker et al., 2010; Geschwind and Levitt, 2007; Minshew and Williams, 2007; Picci et al., 2016), are largely consistent with the notion of ASD as a syndrome due to perturbations of different cytoarchitectonic and neurocognitive systems. According to this view, a reasonable interpretation of our results is that topological organization of interregional GM co-alterations may arise from volumetric aberrations of the regional-level morphology. This hypothesis accords well with the experimental evidence of Ecker et al. (2013), who, performing measures of cortical separation distances on a sample of adults with ASD, reported an abnormal architecture of GM showing reduced cortico-cortical connectivity and low intrinsic wiring costs of the cortex. Interestingly, these authors observed low intrinsic wiring costs in the fronto-posterior areas that are also key components of our MCN, including the left precuneus (BA 7), right temporal pole (BA 22), bilateral orbitofrontal and dorsolateral prefrontal cortices (BA 10, BA 11).

Moreover, our analysis confirms and extends previous results of altered anatomical covariance patterns as a key mechanism in the ASD condition. For example, in the seminal paper of Zielinski et al. (2012), the authors found distributed abnormal components in GM structure using seed-ROIs anchored in the fronto-insular and posterior cingulate cortices. In line with their findings, our data show a non-negligible overlap with pathological covariance sites in ASD. Morphometric components with reduced covariance are clearly present and co-altered in our MCN; some of these are *core* units within the co-alteration pattern. This is the case with regard to the left precuneus, right STG, left supramarginal area, left vACC, left IFG, right MFG, right OFG and the left SFG. Similar results obtained with the same seeds were also reported by Palande et al. (2017), who carried out a graph correlation analysis combined with a statistical inference approach in addition to the anatomical covariance analysis. This general overlap is not surprising, as significant correlations between the MCN and anatomical covariance has been recently evidenced by our group (Cauda et al., 2018a). However, we note that the present methodology differs from the anatomical covariance approach because it enables the examination, in a whole-brain and data-driven manner, of multiple large-scale network affected architectures, thus overcoming the limited resolution of network-level effects given by prior ROI correlations (Evans, 2013; Palande et al., 2017; Tatu et al., 2018; Zielinski et al., 2012).

Another important issue addressed by this study concerns the identification of brain sites that have a pivotal position in the MCN of ASD.

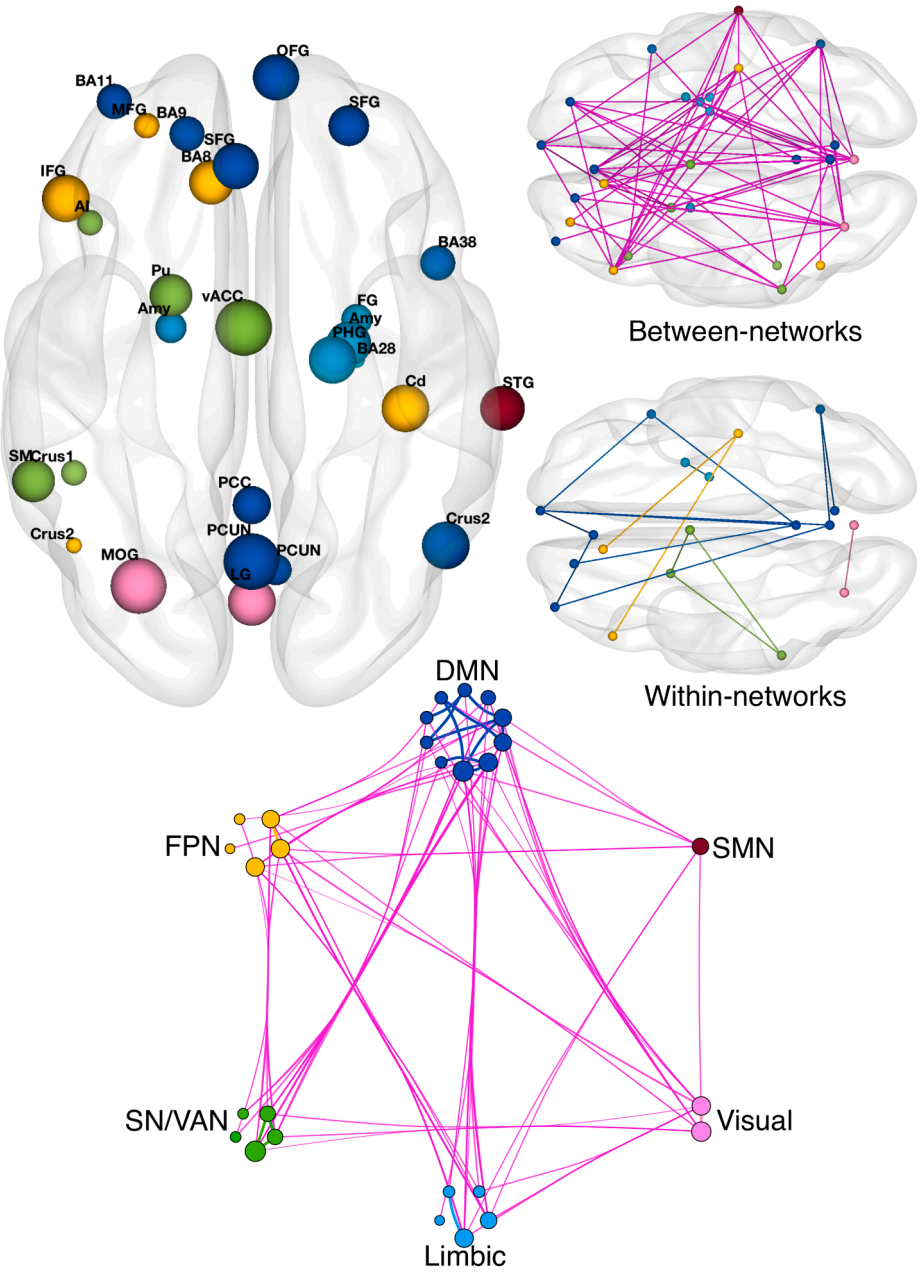

Fig. 6. Brain templates illustrating the anatomical location of the co-altered nodes within the main human large-scale functional networks (left panel) and the between/within network distribution of the co-alterations (right and bottom panels). DMN: default mode network; FPN: frontoparietal network; SN/VAN: salience/ventral attentional network; Limbic: limbic network; Visual: visual network; SMN: sensorimotor network.

Table 3
The network-betweenness of each one of the Yeo et al. (2011) networks. DMN: default mode network; FPN: frontoparietal network; SN/VAN: salience/ventral attentional network; DAN: dorsal attentional network; SMN: sensorimotor network.

Canonical Network	Network Betweenness
DMN	0.82
FPN	0.93
SN/VAN	0.89
DAN	n.a.
Limbic	0.96
Visual	0.95
SMN	1

By combining three different measures of node centrality (i.e., degree, closeness and betweenness), we observe that a subset of areas influences significantly the architecture of co-alterations; for this reason, these multimodal areas can be conceived as pathological hubs (i.e., they are topologically central in the co-alteration network) (Cauda et al., 2018a, 2018b; Manuello et al., 2018). One of those regions is the left precuneus, a component of the medial posterior parietal cortex, which has been frequently associated with social reasoning and self-reflection (Patriquin et al., 2016). The precuneus has also been reported to be involved in a range of integrated tasks, including awareness information processing, visuospatial imagery, mnemonic retrieval and voluntary attention (Cavanna, 2007; Cavanna and Trimble, 2006; Zhang and Li, 2012). From a clinical point of view, its morphometric alterations and decreased functional connectivity have been linked to autistic symptom severity (Cheng et al., 2017; Fang et al., 2020; Lynch et al., 2013), as well as to

dysfunction in mentalizing processes (Wang et al., 2007), attention orienting (Fitzgerald et al., 2015) and empathy (Schulte-Rüther et al., 2011) in different ASD cohorts.

The second pathological hub is the left vACC. Reduced activation of this region has been reported in patients with ASD while playing a social-exchange game (Chiu et al., 2008). Authors have therefore associated this reduced cingulate response with ASD social impairment. Furthermore, it has been observed that developmental differences in the limbic nodes as well as in other integrative regions such as the cingulate cortex might produce a cascading effect on brain areas mediating social perception (Apps et al., 2013; Baron-Cohen et al., 2000; Rolls, 2019). These findings are in agreement with the pattern of our MCN, and with research finding alterations in the activity of the cingulate cortex in individuals with ASD, especially with regard to a reduced glucose metabolism (Haznedar et al., 2000), functional connectivity (Zhou et al., 2016) and disrupted white matter pathways (Barnea-Goraly et al., 2004). It therefore should not be surprising that this region may be significantly co-altered in ASD, given the essential involvement of the vACC in integrative circuits that are supposed to help the regulation of cognitive, executive and emotional processes (for a review see Stevens et al., 2011). Interestingly, the cingulate cortex and the precuneus were proposed to be part of a whole-brain system of areas involved in joint attention, which disruption is an early and characteristic symptom of ASD (Mundy, 2018).

The third hub node identified in the analysis is the left MOG, a second-order region implicated in the integration of multisensory stimuli (Kravitz et al., 2011). It has been recently suggested that microstructural dendritic dispersion of this site is associated with abnormal visual processing in ASD and also with social interaction dysfunction because of its long-range disconnections (Matsuoka et al., 2020). It is worth noting that the central involvement of the MOG in the MCN may indicate an anatomical damage, which can be typical of the ASD condition. As recently reported by VBM transdiagnostic investigations (Cauda et al., 2019b; Liloia et al., 2018), the left portion of the occipital lobe, including BA 18/19, is usually spared by most psychiatric and neurological disorders, and is thereby considered a region with *low structural alteration variety*. Therefore, the present finding further supports the importance of abnormalities at the perceptual level in ASD, as well as of their fronto-posterior patterns. Those abnormalities have been hypothesized to be the basis of sensory aberrations and of failure in socio-communicative integration (Courchesne and Pierce, 2005; Hadjikhani et al., 2004; Lombardo et al., 2019; Marco et al., 2011).

As the aforementioned nodes are also network hubs in the healthy connectome (van den Heuvel and Sporns, 2013), our results are consistent with a recent line of research showing that morphometric damage of brain disorders preferentially accumulates in areas with greater topological value (Crossley et al., 2014), probably due to their long-range connections (Cauda et al., 2020) and related high metabolic cost (Arnatkeviciute et al., 2019a, 2019b; Liang et al., 2013).

We found that the pathological hubs are selectively located in the left hemisphere. Interestingly, this finding is in line with both experimental and theoretical proposals suggesting a typical leftward asymmetry and volumetric reduction in ASD, particularly in cognitive and linguistic-related areas (De Fossé et al., 2004; Floris et al., 2013, 2020; Kong et al., 2020; Mellet et al., 2014; Postema et al., 2019; Prior and Bradshaw, 1979). Moreover, a recent transdiagnostic study from our group (Cauda et al., 2020) found that the regional mean physical distance of co-alteration is higher in the left hemisphere compared to the right one. In other words, the GM decreases of the left hemisphere tend to show long-range co-alterations across many psychiatric and neurological diseases. The concurrent existence of GM decreases and GM increases, which might be taken as evidence of functional and structural failures and compensations, has shown to be more lateralized in the left hemisphere in a range of psychiatric and neurodevelopmental diseases, including autism (Mancuso et al., 2020). Therefore, our current findings of ASD hubs mainly located in left-brain sites suggest a left hemisphere dominance in the co-alteration process.

However, this is not to say that the contribution to the MCN of the right hemisphere is negligible. In fact, there is also an important involvement of right-lateralized sites in the MCN, encompassing the cerebellar crus II, caudate, amygdala, STG and orbitofrontal gyrus. These structures and their dysfunctional connections have attracted much attention in ASD research and have been associated with specific features of social, emotional and motor dysfunctions of the disorder (Bachevalier and Loveland, 2006; D'Mello et al., 2016; D'Mello and Stoodley, 2015; Gibbard et al., 2018; Girgis et al., 2007; Hardan et al., 2006; Qiu et al., 2010; Turner et al., 2006).

To further characterize the topological structure of the MCN and to go beyond the peculiarities of the specific hub nodes, we employed k-core decomposition. Our network clustering analysis suggests that the core hierarchy in ASD contains regions predominantly associated with the highest values of node centrality. In particular, several components are higher-order associative areas, namely left precuneus, left superior and medial frontal gyri, left anterior cingulate cortex, right parahippocampus, along with visual regions such as lingual and middle occipital gyri (Fig. 5). Interestingly, the aforementioned components were recently categorized as units of high hierarchy within large-scale brain networks (Lahav et al., 2016) because they essentially support the structural organization of inter-connections and, thereby, can efficiently allow data integration and monitor cognitive processing (Collin et al., 2014; Hagmann et al., 2008). Thus, our findings support the notion that the integration and monitoring of information might be disrupted in ASD, especially with regard to the social and affective domains associated with the DMN (Buckner and DiNicola, 2019; Padmanabhan et al., 2017), whose nodes appear to be the central components within the MCN of ASD.

Overall, our findings emphasize the importance of the DMN in ASD. In fact, many co-altered nodes have been located in this network, indicating its relevance in the system of reciprocal GM modifications produced by ASD. This is also pointed out by the combined centrality measures and the k-core that highlight brain regions associated with the DMN.

Also, the DMN is the only network whose co-alterations are more likely to be between its nodes and those of other networks than within itself (Fig. 6). This means that the numerous alterations occurring in the DMN also co-occur with many others in the other networks, suggesting a pivotal role of the DMN in the spatial distribution of GM abnormalities in ASD. Despite the fact that direct associations between functional covariation and underlying morphometric substrates remains an open question in autism research (Uddin et al., 2013), the peculiar topology related to the DMN co-alterations might suggest an atypical morphometric substrate for aberrant between-network functional connectivity, which was found decreased in different age-stratified cohorts of individuals with ASD compared with neurotypical controls (Kennedy and Courchesne, 2008; Nomi and Uddin, 2015; von dem Hagen et al., 2013).

Although it is tempting to speculate that the DMN might exert a causal effect in the development of alterations, our analyses do not provide information about the directionality of the co-alteration edges. Still, regardless of the direction of the pathological influence, the central position of the DMN in the pathoconnectome of ASD is significant. By contrast, other networks, namely the SMN and, in particular, the DAN, appeared to be much less involved in our network of co-alterations (Fig. 6 left panel). This seems to indicate that the alterations in these networks do not influence or are not influenced by those in other parts of the brain. It is worth pointing out that the only SMN node is connected to six other nodes spanning across all the remaining networks (Fig. 6 right and bottom panels). Considering its location in the right STG, such a node might be associated with auditory functions, thus suggesting an association between auditory dysfunctions such as hypersensitivity and impaired perception (Marco et al., 2011; Nieto Del Rincón, 2008; Robertson and Baron-Cohen, 2017; Williams et al., 2021). On the contrary,

the lack of edges incident upon the DAN nodes might suggest that any top-down attention deficit of ASD patients (Allen and Courchesne, 2001) might be not associated, at least with respect to morphological substrates, with other symptoms.

Another finding of the present study is a rich pattern of co-alterations related to the limbic nodes including fusiform and orbitofrontal gyri, parahippocampal cortex and amygdar nuclear complex. Disrupted communication of these regions is thought to explain some clinical features of ASD, associated with deficits in emotional processing, social cognition and executive function (Ameis and Catani, 2015; Catani et al., 2016; Haznedar et al., 2000). In particular, the PHG_R node showed high centrality in our results, mostly due to several connections with the DMN. This is not a surprising result, as the parahippocampal gyrus is functionally coupled to the DMN and has been found to be involved in social cognition tasks regarding face versus non-face stimuli (Patriquin et al., 2016). The same brain area has been reported to exhibit altered activity in individuals with ASD during social reward learning task (Choi et al., 2015). These results can be understood in light of the evidence that the memory/encoding system supported by the medial temporal lobe represents a functional subnetwork, which is linked to the cortical nodes of the DMN through parahippocampal connections (Ward et al., 2014).

Another intriguing observation is that the right caudate tends to co-alter with prefrontal areas, encompassing both superior and inferior frontal gyri (i.e., SFG_L, BA8_L and IFG_L). These nodes are components of the dorsolateral prefrontal loop, previously associated with a degraded neuronal organization in ASD (Hashemi et al., 2017; Morgan et al., 2012) and involved in a number of high-order cognitive functions deficient in the disorder, such as complex behavioral planning, working memory processing and procedural learning (Çırak et al., 2020).

Our results also highlighted widespread co-alterations of the cerebellum, both between its hemispheres and through long-range pathways. Converging lines of research offer insight into the link between the cerebellum and ASD symptomatology (Becker and Stoodley, 2013), showing the crucial role of the posterior right lobules and their circuits in core deficits, such as those in language and social cognition processing, stereotyped behaviors and impairments in imitation planning and affective regulation (D'Mello and Stoodley, 2015). Our *meta*-connectomic analysis accords well with these evidences, suggesting a tendency of the Crus2_R to be co-altered with a set of contralateral fronto-posterior nodes (i.e., IFG, MFG, MOG and PCUN) structurally connected and intrinsically implicated in an abnormal cerebro-cerebellar connectivity in mentalizing, verb generation, attention or resting-state tasks (D'Mello and Stoodley, 2015; Ecker et al., 2010; Itahashi et al., 2015; Khan et al., 2015; Noonan et al., 2009; Verly et al., 2014).

The mechanisms that might explain the observed co-alterations are varied. In fact, the presence of an alteration in a brain region might influence another one due to the long-range effects of diaschisis (Carrera and Tononi, 2014), for instance, through the lack of trophic support to the connected regions (Fornito et al., 2015; Nave, 2010; Perlson et al., 2010; Salehi et al., 2003) via direct axonal fiber tracts. In this regard, previous *in vivo* studies suggest that variations in GM morphometry and white matter connectivity are closely linked in ASD (Ameis and Catani, 2015; Andrews et al., 2017; Bos et al., 2015; Ecker et al., 2016; Schaer et al., 2013), reflecting a consistent number of gray-white matter pathological concordances in several clusters throughout the brain (Cauda et al., 2014). Therefore, the correlation between the MCN and structural connectivity might support the hypothesis that connected regions tend to be co-altered because they lack neurotrophic regulation, which has been shown to be essential in normal brain development and maintenance of neuronal connections (Nickl-Jockschat and Michel, 2011). Neurotrophic failure has been also linked to the pathophysiology of ASD (Galvez-Contreras et al., 2017; Garcia et al., 2012; Kasarpalkar et al., 2014; Qin et al., 2016; Zheng et al., 2016), which indicates that a neurotrophic factor mechanism may convincingly explain the formation of the MCN pattern of ASD. Instead, the absence of a significant correlation with the genetic connectivity suggests that a model of shared genetic vulnerability to the disease (Zhou et al., 2012) falls short in explaining the development of the MCN pattern of ASD.

4.1. Methodological considerations and future perspectives

The present *meta*-connectomics analysis proposes a statistically robust view on the GM topology of autism, improving on previous works in several ways. The innovative method used here allowed us to extend spatial information given by canonical CBMAs, providing valuable insights on the mutual relationship between regional changes of the ASD phenotype, as well as on the peculiar role of each aberrant component and of brain connectivity. Also, from a network-level perspective, the MCN integrates current anatomical covariance approaches, exercising a thorough and detailed topological resolution not limited by a prior choice of ROIs or by circumscribed ASD cohort analysis. However, methodologically speaking, it is important to point out that, given the different scale of statistical comparison (i.e., *meta*-analytic vs. group data level), the two types of analysis should not be confused but, rather, integrated for a better comprehension of the dynamic underlying brain disorders. Finally, although this study proposes a new outlook on the ASD brain architecture, the MCN methodology can be potentially applied to any other condition that reflects morphometric disturbances of the brain, opening attractive prospects for an in-depth comprehension of the human pathoconnectome.

Despite these strengths, we acknowledge that some limitations should be recognized. By definition, *meta*-connectomic approaches have general limitations inherent to publication biases (i.e., the file-drawer problem) and to the quality/constraints of individual investigations (Crossley et al., 2016). In this regard, we note that our data set reports a certain degree of heterogeneity in terms of clinical- and age-related differences among participants. Specifically, 23 out of 45 VBM experiments contain a mixed (i.e., comprehensive of two or more diagnostic sub-categories) or an unspecified ASD sample (Table S2). Still, the marked presence of original experimental groups composed of mixed age-stratified participants or with unspecified age ranges (35.6% of the experiments included), hampers the possibility to interpret developmental co-alteration changes in neuroanatomy of ASD (Table S2). In other words, this heterogeneity makes it challenging to discriminate possible differences related to the clinical or age-stratified subpopulations. At the same time, however, it offers important advantages. In fact, in conjunction with the substantial statistical power provided by *meta*-analytic synthesis (Eickhoff et al., 2016), the *meta*-level approach tends to afford more robust and reliable results in terms of generalization for the population of interest (Muller et al., 2018).

Another critical element of the present study relates to the continuous dimensionality of the psychopathology of ASD. Since the diagnosis of ASD includes a wide array of clinical manifestations and biological endophenotypes, it might be pointed out that our database could be affected by a large inter-subject variability. This does not constitute a limitation *per se*, as the aim of a *meta*-analysis is exactly to overcome the heterogeneity of samples in order to discover invariant findings across groups (Tahmasian et al., 2019). However, not considering the peculiarity of each individual or diagnostic subgroup might be simplistic and miss some critical feature of ASD. Future research might develop subject-level methods to assess co-alteration networks, and eventually investigate whether or not they can help discriminate between different categories or dimensions of ASD. At the moment, the main issue to extend the methodology used here to subject-level data is the identification of focal structural alteration in absence of normative intensity values to discriminate between T1 images of healthy and pathological subjects.

The current work does not assess the directionality of the network co-alterations, but future research might test, for instance, the hypothesis that the DMN alterations may play a role in the distribution of the other GM alterations, or the other way round. Finally, the lack of a significant

correlation between the co-alteration network and genetic co-expression connectivity is not indicative of an absence of a genetic role in ASD, but rather, that the genetic influence does not explain the statistical dependence between GM modifications. However, genetic connectivity could have a role in determining the first areas to be affected (Cauda et al., 2019a), while the diaschisis effect might induce other regions to be co-altered (Carrera and Tononi, 2014). Further research is needed to investigate these possibilities.

The long-term aim of the co-alteration approach is to produce valuable insights for clinical practice, in terms of improvement in the diagnostic procedure and in monitoring the disease course. Future investigations may adopt the co-alteration nodes as ROIs to test the generalizability of the MCN pattern on longitudinal native data. In addition, multi-scale research may explore the role of the *meta*-analytic hubs in different clinical cohorts, testing in detail the impact of these key regions on the ASD pathoconnectome. Finally, a more profound comprehension of the role of brain connectivity could help us understand the maladaptive mechanisms underlying the distribution of co-alterations and could pinpoint how to intervene to halt those mechanisms.

5. Conclusion

This study investigated VBM abnormalities of individuals with ASD using a *meta*-connectomic perspective, demonstrating a topologically characteristic structure of co-alteration underlying a circumscribed set of GM sites in the autistic brain. We found that the co-alteration pattern is influenced in part by structural connectivity, which is in line with the hypothesis that the brain connectome plays an important role in the development of disease-related alterations. Finally, we observed that the regions belonging to the DMN are central in the topology of co-alterations, thus suggesting a significant contribution of DMN dysfunction in the pathophysiology of ASD. This effect may be due to the strong network-betweenness of the DMN, which makes GM alterations in these network regions to be pathoconnectivity centers. In conclusion, the present study provides new insight into the complex pathophysiology of ASD, emphasizing the need for a more integrative view based on large-scale network dysfunction in order to better understand the complex clinical manifestations of this spectrum of disorders.

6. Funding information

This study was supported by Fondazione SanPaolo, Turin (Cauda F. PI)

CRediT authorship contribution statement

Donato Liloia: Conceptualization, Methodology, Formal analysis, Investigation, Resources, Data curation, Writing - original draft, Writing - review & editing, Visualization. **Lorenzo Mancuso:** Formal analysis, Investigation, Writing - original draft, Writing - review & editing. **Lucina Q. Uddin:** Writing - review & editing. **Tommaso Costa:** Methodology, Software, Formal analysis, Validation, Supervision. **Andrea Nani:** Writing - review & editing. **Roberto Keller:** Writing - review & editing. **Jordi Manuello:** Formal analysis, Writing - review & editing. **Sergio Duca:** Project administration. **Franco Cauda:** Conceptualization, Data curation, Writing - review & editing, Supervision, Project administration, Funding acquisition.

Declaration of Competing Interest

The authors declare that they have no known competing financial interests or personal relationships that could have appeared to influence the work reported in this paper.

Acknowledgments

Data were provided [in part: diffusion tensor imaging (DTI) data set] by the Human Connectome Project, WU-Minn Consortium (Principal Investigators: David Van Essen and Kamil Ugurbil; 1U54MH091657) funded by the 16 NIH Institutes and Centers that support the NIH Blueprint for Neuroscience Research; and by the McDonnell Center for Systems Neuroscience at Washington University.

Appendix A. Supplementary data

Supplementary data to this article can be found online at https://doi.org/10.1016/j.nicl.2021.102583.

References

Ajilore, O., Vizueta, N., Walshaw, P., Zhan, L., Leow, A., Altshuler, L.L., 2015. Connectome signatures of neurocognitive abnormalities in euthymic bipolar I disorder. J. Psychiatr. Res. 68, 37–44. https://doi.org/10.1016/j.jpsychires.2015.05.017.

Alexander-Bloch, A., Giedd, J.N., Bullmore, E.d., 2013. Imaging structural co-variance between human brain regions. Nat. Rev. Neurosci. 14 (5), 322–336. https://doi.org/10.1038/nrn3465.

Allen, G., Courchesne, E., 2001. Attention function and dysfunction in autism. Front. Biosci. 6, D105–D119. https://doi.org/10.2741/allen.

Ameis, S.H., Catani, M., 2015. Altered white matter connectivity as a neural substrate for social impairment in Autism Spectrum Disorder. Cortex 62, 158–181. https://doi.org/10.1016/j.cortex.2014.10.014.

American Psychiatric Association, 2013. Diagnostic and Statistical Manual of Mental Disorders, Fifth Edition (DSM-5), 5th, ed. American Psychiatric Publishing, Arlington, VA.

Andrews, D.S., Avino, T.A., Gudbrandsen, M., Daly, E., Marquand, A., Murphy, C.M., Lai, M.C., Lombardo, M.V., Ruigrok, A.N., Williams, S.C., Bullmore, E.T., The Mrc Aims, C., Suckling, J., Baron-Cohen, S., Craig, M.C., Murphy, D.G., Ecker, C., 2017. In Vivo Evidence of Reduced Integrity of the Gray-White Matter Boundary in Autism Spectrum Disorder. Cereb Cortex 27, 877-887. doi: 10.1093/cercor/bhw404.

Apps, M.A., Lockwood, P.L., Balsters, J.H., 2013. The role of the midcingulate cortex in monitoring others' decisions. Front. Neurosci. 7, 251. https://doi.org/10.3389/fnins.2013.00251.

Arnatkeviciute, A., Fulcher, B.D., Fornito, A., 2019a. A practical guide to linking brain-wide gene expression and neuroimaging data. Neuroimage 189, 353–367. https://doi.org/10.1016/j.neuroimage.2019.01.011.

Arnatkeviciute, A., Fulcher, B.D., Fornito, A., 2019b. Uncovering the transcriptional correlates of hub connectivity in neural networks. Front. Neural Circuits 13, 47. https://doi.org/10.3389/fncir.2019.00047.

Ashburner, J., Friston, K.J., 2000. Voxel-based morphometry—the methods. Neuroimage 11 (6), 805–821. https://doi.org/10.1006/nimg.2000.0582.

Ashburner, J., Friston, K.J., 2001. Why voxel-based morphometry should be used. Neuroimage 14 (6), 1238–1243. https://doi.org/10.1006/nimg.2001.0961.

Bachevalier, J., Loveland, K.A., 2006. The orbitofrontal-amygdala circuit and self-regulation of social-emotional behavior in autism. Neurosci. Biobehav. Rev. 30 (1), 97–117. https://doi.org/10.1016/j.neubiorev.2005.07.002.

Baio, J., Wiggins, L., Christensen, D.L., Maenner, M.J., Daniels, J., Warren, Z., Kurzius-Spencer, M., Zahorodny, W., Robinson, C., Rosenberg, White, T., Durkin, M.S., Imm, P., Nikolaou, L., Yeargin-Allsopp, M., Lee, L.-C., Harrington, R., Lopez, M., Fitzgerald, R.T., Hewitt, A., Pettygrove, S., Constantino, J.N., Vehorn, A., Shenouda, J., Hall-Lande, J., Van, K., Naarden, Braun, Dowling, N.F., 2018. Prevalence of Autism Spectrum Disorder Among Children Aged 8 Years - Autism and Developmental Disabilities Monitoring Network, 11 Sites, United States, 2014. MMWR Surveill Summ 67 (6), 1–23. https://doi.org/10.15585/mmwr.ss6706a1.

Balardin, J.B., Comfort, W.E., Daly, E., Murphy, C., Andrews, D., Murphy, D.G., Ecker, C., Sato, J.R., 2015. Decreased centrality of cortical volume covariance networks in autism spectrum disorders. J. Psychiatr. Res. 69, 142–149. https://doi.org/10.1016/j.jpsychires.2015.08.003.

Barnea-Goraly, N., Kwon, H., Menon, V., Eliez, S., Lotspeich, L., Reiss, A.L., 2004. White matter structure in autism: preliminary evidence from diffusion tensor imaging. Biol. Psychiatry 55 (3), 323–326. https://doi.org/10.1016/j.biopsych.2003.10.022.

Baron-Cohen, S., Ring, H.A., Bullmore, E.T., Wheelwright, S., Ashwin, C., Williams, S.C. R., 2000. The amygdala theory of autism. Neurosci. Biobehav. Rev. 24 (3), 355–364. https://doi.org/10.1016/S0149-7634(00)00011-7.

Becker, E.B., Stoodley, C.J., 2013. Autism spectrum disorder and the cerebellum. Int. Rev. Neurobiol. 113, 1–34. https://doi.org/10.1016/B978-0-12-418700-9.00001-0.

Bernhardt, B.C., Valk, S.L., Silani, G., Bird, G., Frith, U., Singer, T., 2014. Selective disruption of sociocognitive structural brain networks in autism and alexithymia. Cereb. Cortex 24, 3258–3267. https://doi.org/10.1093/cercor/bht182.

Bethlehem, R.A.I., Romero-Garcia, R., Mak, E., Bullmore, E.T., Baron-Cohen, S., 2017. Structural covariance networks in children with autism or ADHD. Cereb. Cortex 27, 4267–4276. https://doi.org/10.1093/cercor/bhx135.

Bolland, J.M., 1988. Sorting out centrality: An analysis of the performance of four centrality models in real and simulated networks. Social Networks 10 (3), 233–253. https://doi.org/10.1016/0378-8733(88)90014-7.

Bos, D.J., Merchán-Naranjo, J., Martínez, K., Pina-Camacho, L., Balsa, I., Boada, L., Schnack, H., Oranje, B., Desco, M., Arango, C., Parellada, M., Durston, S., Janssen, J., 2015. Reduced gyrification is related to reduced interhemispheric connectivity in autism spectrum disorders. J. Am. Acad. Child Adolesc. Psychiatry 54 (8), 668–676. https://doi.org/10.1016/j.jaac.2015.05.011.

Brighenti, S., Schintu, S., Liloia, D., Keller, R., 2018. Neuropsychological aspects of Asperger Syndrome in adults: a review. Neuropsychological Trends (24), 63–95. https://doi.org/10.7358/neur-2018-024-brig.

Buckholtz, J., Meyer-Lindenberg, A., 2012. Psychopathology and the human connectome: toward a transdiagnostic model of risk for mental illness. Neuron 74 (6), 990–1004. https://doi.org/10.1016/j.neuron.2012.06.002.

Buckner, R.L., DiNicola, L.M., 2019. The brain's default network: updated anatomy, physiology and evolving insights. Nat. Rev. Neurosci. 20 (10), 593–608. https://doi.org/10.1038/s41583-019-0212-7.

Buckner, R.L., Krienen, F.M., Castellanos, A., Diaz, J.C., Yeo, B.T.T., 2011. The organization of the human cerebellum estimated by intrinsic functional connectivity. J. Neurophysiol. 106 (5), 2322–2345. https://doi.org/10.1152/jn.00339.2011.

Bullmore, E.d., Sporns, O., 2012. The economy of brain network organization. Nat. Rev. Neurosci. 13 (5), 336–349. https://doi.org/10.1038/nrn3214.

Butts, C.T., 2009. Revisiting the foundations of network analysis. Science 325 (5939), 414–416. https://doi.org/10.1126/science:1171022.

Cao, M., Wang, Z., He, Y., 2015. Connectomics in psychiatric research: advances and applications. Neuropsychiatr. Dis. Treat. 11, 2801–2810. https://doi.org/10.2147/ndt.s63470.

Cao, R., Yang, X., Luo, J., Wang, P., Meng, F., Xia, M., He, Y., Zhao, T., Li, Z., 2021. The effects of cognitive behavioral therapy on the whole brain structural connectome in unmedicated patients with obsessive-compulsive disorder. Prog. Neuro-Psychopharmacol. Biol. Psychiatry 104, 110037. https://doi.org/10.1016/j.pnpbp.2020.110037.

Cardon, G.J., Hepburn, S., Rojas, D.C., 2017. Structural Covariance of Sensory Networks, the Cerebellum, and Amygdala in Autism Spectrum Disorder. Front. Neurol. 8, 615. https://doi.org/10.3389/fneur.2017.00615.

Carlisi, C.O., Norman, L.J., Lukito, S.S., Radua, J., Mataix-Cols, D., Rubia, K., 2017. Comparative multimodal meta-analysis of structural and functional brain abnormalities in autism spectrum disorder and obsessive-compulsive disorder. Biol. Psychiatry 82 (2), 83–102. https://doi.org/10.1016/j.biopsych.2016.10.006.

Carrera, E., Tononi, G., 2014. Diaschisis: past, present, future. Brain 137, 2408–2422. https://doi.org/10.1093/brain/awu101.

Casanova, M.F., 2006. Neuropathological and genetic findings in autism: the significance of a putative minicolumnopathy. Neuroscientist 12 (5), 435–441. https://doi.org/10.1177/1073858406290375.

Catani, M., Dell'Acqua, F., Budisavljevic, S., Howells, H., Thiebaut de Schotten, M., Froudist-Walsh, S., D'Anna, L., Thompson, A., Sandrone, S., Bullmore, E.T., Suckling, J., Baron-Cohen, S., Lombardo, M.V., Wheelwright, S.J., Chakrabarti, B., Lai, M.-C., Ruigrok, A.N.V., Leemans, A., Ecker, C., Consortium, MRC.AIMS., Craig, M.C., Murphy, D.G.M., 2016. Frontal networks in adults with autism spectrum disorder. Brain 139 (2), 616–630. https://doi.org/10.1093/brain/awv351.

Cauda, F., Costa, T., Palermo, S., D'Agata, F., Diano, M., Bianco, F., Duca, S., Keller, R., 2014. Concordance of white matter and gray matter abnormalities in autism spectrum disorders: a voxel-based meta-analysis study. Hum. Brain Mapp. 35 (5), 2073–2098. https://doi.org/10.1002/hbm.22313.

Cauda, F., Geda, E., Sacco, K., D'Agata, F., Duca, S., Geminiani, G., Keller, R., 2011. Grey matter abnormality in autism spectrum disorder: an activation likelihood estimation meta-analysis study. J. Neurol. Neurosurg. Psychiatry 82 (12), 1304–1313. https://doi.org/10.1136/jnnp.2010.239111.

Cauda, F., Mancuso, L., Nani, A., Costa, T., 2019a. Heterogeneous neuroimaging findings, damage propagation and connectivity: an integrative view. e17 Brain 142, e17. https://doi.org/10.1093/brain/awz080.

Cauda, F., Mancuso, L., Nani, A., Ficco, L., Premi, E., Manuello, J., Liloia, D., Gelmini, G., Duca, S., Costa, T., 2020. Hubs of long-distance co-alteration characterize brain pathology. Hum. Brain Mapp. 41 (14), 3878–3899. https://doi.org/10.1002/hbm.v41.1410.1002/hbm.25093.

Cauda, F., Nani, A., Costa, T., Palermo, S., Tatu, K., Manuello, J., Duca, S., Fox, P.T., Keller, R., 2018a. The morphometric co-atrophy networking of schizophrenia, autistic and obsessive spectrum disorders. Hum. Brain Mapp. 39 (5), 1898–1928. https://doi.org/10.1002/hbm.23952.

Cauda, F., Nani, A., Manuello, J., Liloia, D., Tatu, K., Vercelli, U., Duca, S., Fox, P.T., Costa, T., 2019b. The alteration landscape of the cerebral cortex. Neuroimage 184, 359–371. https://doi.org/10.1016/j.neuroimage.2018.09.036.

Cauda, F., Nani, A., Manuello, J., Premi, E., Palermo, S., Tatu, K., Duca, S., Fox, P.T., Costa, T., 2018b. Brain structural alterations are distributed following functional, anatomic and genetic connectivity. Brain 141, 3211–3232. https://doi.org/10.1093/brain/awy252.

Cavanna, A.E., 2007. The precuneus and consciousness. CNS Spectr. 12 (7), 545–552. https://doi.org/10.1017/S1092852900021295.

Cavanna, A.E., Trimble, M.R., 2006. The precuneus: a review of its functional anatomy and behavioural correlates. Brain 129, 564–583. https://doi.org/10.1093/brain/awl004.

Cheng, W., Rolls, E.T., Zhang, J., Sheng, W., Ma, L., Wan, L., Luo, Q., Feng, J., 2017. Functional connectivity decreases in autism in emotion, self, and face circuits identified by Knowledge-based Enrichment Analysis. Neuroimage 148, 169–178. https://doi.org/10.1016/j.neuroimage.2016.12.068.

Chiu, P.H., Kayali, M.A., Kishida, K.T., Tomlin, D., Klinger, L.G., Klinger, M.R., Montague, P.R., 2008. Self responses along cingulate cortex reveal quantitative neural phenotype for high-functioning autism. Neuron 57 (3), 463–473. https://doi.org/10.1016/j.neuron.2007.12.020.

Choi, E.Y., Yeo, B.T.T., Buckner, R.L., 2012. The organization of the human striatum estimated by intrinsic functional connectivity. J. Neurophysiol. 108 (8), 2242–2263. https://doi.org/10.1152/jn.00270.2012.

Choi, U.S., Kim, S.Y., Sim, H.J., Lee, S.Y., Park, S.Y., Jeong, J.S., Seol, K.I., Yoon, H.W., Jhung, K., Park, J.I., Cheon, K.A., 2015. Abnormal brain activity in social reward learning in children with autism spectrum disorder: an fMRI study. Yonsei Med. J. 56, 705–711. https://doi.org/10.3349/ymj.2015.56.3.705.

Çırak, M., Yağmurlu, K., Kearns, K.N., Ribas, E.C., Urgun, K., Shaffrey, M.E., Kalani, M.Y. S., 2020. The Caudate Nucleus: Its Connections, Surgical Implications, and Related Complications. World Neurosurg 139, e428–e438. https://doi.org/10.1016/j.wneu.2020.04.027.

Collin, G., Sporns, O., Mandl, R.C.W., van den Heuvel, M.P., 2014. Structural and functional aspects relating to cost and benefit of rich club organization in the human cerebral cortex. Cereb. Cortex 24 (9), 2258–2267. https://doi.org/10.1093/cercor/bht064.

Collin, G., van den Heuvel, M.P., Abramovic, L., Vreeker, A., de Reus, M.A., van Haren, N.E.M., Boks, M.P.M., Ophoff, R.A., Kahn, R.S., 2016. Brain network analysis reveals affected connectome structure in bipolar I disorder. Hum. Brain Mapp. 37 (1), 122–134. https://doi.org/10.1002/hbm.23017.

Courchesne, E., Pierce, K., 2005. Why the frontal cortex in autism might be talking only to itself: local over-connectivity but long-distance disconnection. Curr. Opin. Neurobiol. 15 (2), 225–230. https://doi.org/10.1016/j.conb.2005.03.001.

Crossley, N.A., Fox, P.T., Bullmore, E.T., 2016. Meta-connectomics: human brain network and connectivity meta-analyses. Psychol. Med. 46 (5), 897–907. https://doi.org/10.1017/S0033291715002895.

Crossley, N.A., Mechelli, A., Scott, J., Carletti, F., Fox, P.T., McGuire, P., Bullmore, E.T., 2014. The hubs of the human connectome are generally implicated in the anatomy of brain disorders. Brain 137, 2382–2395. https://doi.org/10.1093/brain/awu132.

D'Mello, A.M., Moore, D.M., Crocetti, D., Mostofsky, S.H., Stoodley, C.J., 2016. Cerebellar gray matter differentiates children with early language delay in autism. Autism Res. 9 (11), 1191–1204. https://doi.org/10.1002/aur.2016.9.issue-1110.1002/aur.1622.

D'Mello, A.M., Stoodley, C.J., 2015. Cerebro-cerebellar circuits in autism spectrum disorder. Front. Neurosci. 9, 408. https://doi.org/10.3389/fnins.2015.00408.

De Fossé, L., Hodge, S.M., Makris, N., Kennedy, D.N., Caviness, V.S., McGrath, L., Steele, S., Ziegler, D.A., Herbert, M.R., Frazier, J.A., Tager-Flusberg, H., Harris, G.J., 2004. Language-association cortex asymmetry in autism and specific language impairment. Ann. Neurol. 56 (6), 757–766. https://doi.org/10.1002/ana.20275.

Deco, G., Kringelbach, M., 2014. Great expectations: using whole-brain computational connectomics for understanding neuropsychiatric disorders. Neuron 84 (5), 892–905. https://doi.org/10.1016/j.neuron.2014.08.034.

DeRamus, T.P., Kana, R.K., 2015. Anatomical likelihood estimation meta-analysis of grey and white matter anomalies in autism spectrum disorders. Neuroimage Clin. 7, 525–536. https://doi.org/10.1016/j.nicl.2014.11.004.

Ecker, C., Andrews, D., Dell'Acqua, F., Daly, E., Murphy, C., Catani, M., Thiebaut de Schotten, M., Baron-Cohen, S., Lai, M.C., Lombardo, M.V., Bullmore, E.T., Suckling, J., Williams, S., Jones, D.K., Chiocchetti, A., Murphy, D.G.M., 2016. Relationship between cortical gyrification, white matter connectivity, and autism spectrum disorder. Cereb. Cortex 26 (7), 3297–3309. https://doi.org/10.1093/cercor/bhw098.

Ecker, C., Bookheimer, S.Y., Murphy, D.G.M., 2015. Neuroimaging in autism spectrum disorder: brain structure and function across the lifespan. Lancet Neurol. 14 (11), 1121–1134. https://doi.org/10.1016/S1474-4422(15)00050-2.

Ecker, C., Rocha-Rego, V., Johnston, P., Mourao-Miranda, J., Marquand, A., Daly, E.M., Brammer, M.J., Murphy, C., Murphy, D.G., 2010. Investigating the predictive value of whole-brain structural MR scans in autism: a pattern classification approach. Neuroimage 49 (1), 44–56. https://doi.org/10.1016/j.neuroimage.2009.08.024.

Ecker, C., Ronan, L., Feng, Y., Daly, E., Murphy, C., Ginestet, C.E., Brammer, M., Fletcher, P.C., Bullmore, E.T., Suckling, J., Baron-Cohen, S., Williams, S., Loth, E., Murphy, D.G.M., Bailey, A.J., Baron-Cohen, S., Bolton, P.F., Bullmore, E.T., Carrington, S., Chakrabarti, B., Daly, E.M., Deoni, S.C., Ecker, C., Happe, F., Henty, J., Jezzard, P., Johnston, P., Jones, D.K., Lai, M.C., Lombardo, M.V., Madden, A., Mullins, D., Murphy, C.M., Murphy, D.G., Pasco, G., Sadek, S., Spain, D., Steward, R., Suckling, J., Wheelwright, S., Williams, S.C., 2013. Intrinsic gray-matter connectivity of the brain in adults with autism spectrum disorder. Proc. Natl. Acad. Sci. U.S.A. 110 (32), 13222–13227. https://doi.org/10.1073/pnas.1221880110.

Eickhoff, S.B., Bzdok, D., Laird, A.R., Kurth, F., Fox, P.T., 2012. Activation likelihood estimation meta-analysis revisited. Neuroimage 59 (3), 2349–2361. https://doi.org/10.1016/j.neuroimage.2011.09.017.

Eickhoff, S.B., Laird, A.R., Grefkes, C., Wang, L.E., Zilles, K., Fox, P.T., 2009. Coordinate-based activation likelihood estimation meta-analysis of neuroimaging data: a random-effects approach based on empirical estimates of spatial uncertainty. Hum. Brain Mapp. 30 (9), 2907–2926. https://doi.org/10.1002/hbm.v30:910.1002/hbm.20718.

Eickhoff, S.B., Nichols, T.E., Laird, A.R., Hoffstaedter, F., Amunts, K., Fox, P.T., Bzdok, D., Eickhoff, C.R., 2016. Behavior, sensitivity, and power of activation likelihood estimation characterized by massive empirical simulation. Neuroimage 137, 70–85. https://doi.org/10.1016/j.neuroimage.2016.04.072.

Eisenberg, I.W., Wallace, G.L., Kenworthy, L., Gotts, S.J., Martin, A., 2015. Insistence on sameness relates to increased covariance of gray matter structure in autism spectrum disorder. Mol. Autism 6, 54. https://doi.org/10.1186/s13229-015-0047-7.

Evans, A.C., 2013. Networks of anatomical covariance. Neuroimage 80, 489–504. https://doi.org/10.1016/j.neuroimage.2013.05.054.

Fang, H., Wu, Q., Li, Y., Ren, Y., Li, C., Xiao, X., Xiao, T., Chu, K., Ke, X., 2020. Structural networks in children with autism spectrum disorder with regression: a graph theory study. Behav. Brain Res. 378, 112262. https://doi.org/10.1016/j.bbr.2019.112262.

Fernandes, H.M., Cabral, J., van Hartevelt, T.J., Lord, L.D., Gleesborg, C., Møller, A., Deco, G., Whybrow, P.C., Petrovic, P., James, A.C., Kringelbach, M.L., 2019. Disrupted brain structural connectivity in Pediatric Bipolar Disorder with psychosis. Sci. Rep. 9, 13638. https://doi.org/10.1038/s41598-019-50093-4.

Filippi, M., van den Heuvel, M.P., Fornito, A., He, Y., Hulshoff Pol, H.E., Agosta, F., Comi, G., Rocca, M.A., 2013. Assessment of system dysfunction in the brain through MRI-based connectomics. Lancet Neurol. 12 (12), 1189–1199. https://doi.org/10.1016/S1474-4422(13)70144-3.

Fitzgerald, J., Johnson, K., Kehoe, E., Bokde, A.L.W., Garavan, H., Gallagher, L., McGrath, J., 2015. Disrupted functional connectivity in dorsal and ventral attention networks during attention orienting in autism spectrum disorders. Autism Res 8 (2), 136–152. https://doi.org/10.1002/aur.1430.

Floris, D.L., Chura, L.R., Holt, R.J., Suckling, J., Bullmore, E.T., Baron-Cohen, S., Spencer, M.D., 2013. Psychological correlates of handedness and corpus callosum asymmetry in autism: the left hemisphere dysfunction theory revisited. J. Autism Dev. Disord. 43 (8), 1758–1772. https://doi.org/10.1007/s10803-012-1720-8.

Floris, D.L., Wolfers, T., Zabihi, M., Holz, N.E., Zwiers, M.P., Charman, T., Tillmann, J., Ecker, C., Dell'Acqua, F., Banaschewski, T., Moessnang, C., Baron-Cohen, S., Holt, R., Durston, S., Loth, E., Murphy, D., Marquand, A., Buitelaar, J.K., Beckmann, C.F., 2020. Atypical brain asymmetry in autism – a candidate for clinically meaningful stratification. Biological Psychiatry: Cognitive Neuroscience and Neuroimaging. doi: 10.1016/j.bpsc.2020.08.008.

Fornito, A., Bullmore, E.T., 2015. Connectomics: a new paradigm for understanding brain disease. Eur. Neuropsychopharmacol. 25 (5), 733–748. https://doi.org/10.1016/j.euroneuro.2014.02.011.

Fornito, A., Bullmore, E.T., Zalesky, A., 2017. Opportunities and Challenges for Psychiatry in the Connectomic Era. Biol Psychiatry Cogn Neurosci Neuroimaging 2 (1), 9–19. https://doi.org/10.1016/j.bpsc.2016.08.003.

Fornito, A., Zalesky, A., Breakspear, M., 2015. The connectomics of brain disorders. Nat. Rev. Neurosci. 16 (3), 159–172. https://doi.org/10.1038/nrn3901.

Fornito, A., Zalesky, A., Bullmore, E., 2016. Fundamentals of brain network analysis. Academic Press.

Fox, P.T., Laird, A.R., Fox, S.P., Fox, P.M., Uecker, A.M., Crank, M., Koenig, S.F., Lancaster, J.L., 2005. BrainMap taxonomy of experimental design: description and evaluation. Hum. Brain Mapp. 25 (1), 185–198. https://doi.org/10.1002/(ISSN)1097-019310.1002/hbm.v25:110.1002/hbm.20141.

Freeman, L.C., 1978. Centrality in social networks: conceptual clarification. Social networks 1 (3), 215–239. https://doi.org/10.1016/0378-8733(78)90021-7.

Frith, C., 2004. Is autism a disconnection disorder? Lancet Neurol. 3 (10), 577. https://doi.org/10.1016/S1474-4422(04)00875-0.

Galvez-Contreras, A.Y., Campos-Ordonez, T., Gonzalez-Castaneda, R.E., Gonzalez-Perez, O., 2017. Alterations of Growth Factors in Autism and Attention-Deficit/Hyperactivity Disorder. Front. Psychiatry 8. https://doi.org/10.3389/fpsyt.2017.00126.

Garcia, K.L.P., Yu, G., Nicolini, C., Michalski, B., Garzon, D.J., Chiu, V.S., Tongiorgi, E., Szatmari, P., Fahnestock, M., 2012. Altered balance of proteolytic isoforms of pro-brain-derived neurotrophic factor in autism. J. Neuropathol. Exp. Neurol. 71 (4), 289–297. https://doi.org/10.1097/NEN.0b013e31824b27e4.

Geschwind, D.H., Levitt, P., 2007. Autism spectrum disorders: developmental disconnection syndromes. Curr. Opin. Neurobiol. 17 (1), 103–111. https://doi.org/10.1016/j.conb.2007.01.009.

Gibbard, C.R., Ren, J., Skuse, D.H., Clayden, J.D., Clark, C.A., 2018. Structural connectivity of the amygdala in young adults with autism spectrum disorder. Hum. Brain Mapp. 39 (3), 1270–1282. https://doi.org/10.1002/hbm.23915.

Girgis, R.R., Minshew, N.J., Melhem, N.M., Nutche, J.J., Keshavan, M.S., Hardan, A.Y., 2007. Volumetric alterations of the orbitofrontal cortex in autism. Prog. Neuro-Psychopharmacol. Biol. Psychiatry 31 (1), 41–45. https://doi.org/10.1016/j.pnpbp.2006.06.007.

Goodkind, M., Eickhoff, S.B., Oathes, D.J., Jiang, Y., Chang, A., Jones-Hagata, L.B., Ortega, B.N., Zaiko, Y.V., Roach, E.L., Korgaonkar, M.S., Grieve, S.M., Galatzer-Levy, I., Fox, P.T., Etkin, A., 2015. Identification of a common neurobiological substrate for mental illness. JAMA Psychiatry 72, 305–315. https://doi.org/10.1001/jamapsychiatry.2014.2206.

Grecucci, A., Rubicondo, D., Siugzdaite, R., Surian, L., Job, R., 2016. Uncovering the social deficits in the autistic brain. A source-based morphometric study. Front. Neurosci. 10, 388. https://doi.org/10.3389/fnins.2016.00388.

Hadjikhani, N., Chabris, C.F., Joseph, R.M., Clark, J., McGrath, L., Aharon, I., Feczko, E., Tager-Flusberg, H., Harris, G.J., 2004. Early visual cortex organization in autism: an fMRI study. NeuroReport 15 (2), 267–270. https://doi.org/10.1097/00001756-200402090-00011.

Hagmann, P., Cammoun, L., Gigandet, X., Meuli, R., Honey, C.J., Wedeen, V.J., Sporns, O., Friston, K.J., 2008. Mapping the structural core of human cerebral cortex. PLoS Biol. 6 (7), e159. https://doi.org/10.1371/journal.pbio.0060159.

Hardan, A.Y., Girgis, R.R., Lacerda, A.L.T., Yorbik, O., Kilpatrick, M., Keshavan, M.S., Minshew, N.J., 2006. Magnetic resonance imaging study of the orbitofrontal cortex in autism. J. Child Neurol. 21 (10), 866–871. https://doi.org/10.1177/08830738060210100701.

Hashemi, E., Ariza, J., Rogers, H., Noctor, S.C., Martínez-Cerdeño, V., 2017. The number of parvalbumin-expressing interneurons is decreased in the prefrontal cortex in autism. Cereb. Cortex 27, 1931–1943. https://doi.org/10.1093/cercor/bhw021.

Hawrylycz, M.J., Lein, E.S., Guillozet-Bongaarts, A.L., Shen, E.H., Ng, L., Miller, J.A., van de Lagemaat, L.N., Smith, K.A., Ebbert, A., Riley, Z.L., Abajian, C., Beckmann, C.F., Bernard, A., Bertagnolli, D., Boe, A.F., Cartagena, P.M., Chakravarty, M.M., Chapin, M., Chong, J., Dalley, R.A., Daly, B.D., Dang, C., Datta, S., Dee, N., Dolbeare, T.A., Faber, V., Feng, D., Fowler, D.R., Goldy, J., Gregor, B.W., Haradon, Z., Haynor, D.R., Hohmann, J.G., Horvath, S., Howard, R.E., Jeromin, A., Jochim, J.M., Kinnunen, M., Lau, C., Lazarz, E.T., Lee, C., Lemon, T.A., Li, L., Li, Y., Morris, J.A., Overly, C.C., Parker, P.D., Parry, S.E., Reding, M., Royall, J.J., Schulkin, J., Sequeira, P.A., Slaughterbeck, C.R., Smith, S.C., Sodt, A.J., Sunkin, S.M., Swanson, B.E., Vawter, M.P., Williams, D., Wohnoutka, P., Zielke, H.R., Geschwind, D.H., Hof, P.R., Smith, S.M., Koch, C., Grant, S.G.N., Jones, A.R., 2012. An anatomically comprehensive atlas of the adult human brain transcriptome. Nature 489 (7416), 391–399. https://doi.org/10.1038/nature11405.

Hawrylycz, M., Miller, J.A., Menon, V., Feng, D., Dolbeare, T., Guillozet-Bongaarts, A.L., Jegga, A.G., Aronow, B.J., Lee, C.-K., Bernard, A., Glasser, M.F., Dierker, D.L., Menche, J., Szafer, A., Collman, F., Grange, P., Berman, K.A., Mihalas, S., Yao, Z., Stewart, L., Barabási, A.-L., Schulkin, J., Phillips, J., Ng, L., Dang, C., Haynor, D.R., Jones, A., Van Essen, D.C., Koch, C., Lein, E.d., 2015. Canonical genetic signatures of the adult human brain. Nat. Neurosci. 18 (12), 1832–1844. https://doi.org/10.1038/nn.4171.

Haznedar, M.M., Buchsbaum, M.S., Wei, T.-C., Hof, P.R., Cartwright, C., Bienstock, C.A., Hollander, E., 2000. Limbic circuitry in patients with autism spectrum disorders studied with positron emission tomography and magnetic resonance imaging. Am. J. Psychiatry 157 (12), 1994–2001. https://doi.org/10.1176/appi.ajp.157.12.1994.

Huys, Q.J.M., Maia, T.V., Frank, M.J., 2016. Computational psychiatry as a bridge from neuroscience to clinical applications. Nat. Neurosci. 19 (3), 404–413. https://doi.org/10.1038/nn.4238.

Insel, T., Cuthbert, B., Garvey, M., Heinssen, R., Pine, D.S., Quinn, K., Sanislow, C., Wang, P., 2010. Research domain criteria (RDoC): toward a new classification framework for research on mental disorders. Am. J. Psychiatry 167 (7), 748–751. https://doi.org/10.1176/appi.ajp.2010.09091379.

Insel, T.R., 2014. The NIMH Research Domain Criteria (RDoC) Project: precision medicine for psychiatry. Am. J. Psychiatry 171 (4), 395–397. https://doi.org/10.1176/appi.ajp.2014.14020138.

Itahashi, T., Yamada, T., Watanabe, H., Nakamura, M., Ohta, H., Kanai, C., Iwanami, A., Kato, N., Hashimoto, R., 2015. Alterations of local spontaneous brain activity and connectivity in adults with high-functioning autism spectrum disorder. Mol. Autism 6, 30. https://doi.org/10.1186/s13229-015-0026-z.

Iturria-Medina, Y., Evans, A.C., 2015. On the central role of brain connectivity in neurodegenerative disease progression. Front. Aging Neurosci. 7, 90. https://doi.org/10.3389/fnagi.2015.00090.

Kasarpalkar, N.J., Kothari, S.T., Dave, U.P., 2014. Brain-derived neurotrophic factor in children with autism spectrum disorder. Ann Neurosci 21, 129–133. https://doi.org/10.5214/ans.0972.7531.210403.

Keller, R., Chieregato, S., Bari, S., Castaldo, R., Rutto, F., Chiocchetti, A., Dianzani, U., 2020. Autism in adulthood: clinical and demographic characteristics of a cohort of five hundred persons with autism analyzed by a novel multistep network model. Brain Sci. 10 (7), 416. https://doi.org/10.3390/brainsci10070416.

Kennedy, D.P., Courchesne, E., 2008. Functional abnormalities of the default network during self- and other-reflection in autism. Soc. Cogn. Affect Neurosci. 3 (2), 177–190. https://doi.org/10.1093/scan/nsn011.

Khan, A.J., Nair, A., Keown, C.L., Datko, M.C., Lincoln, A.J., Müller, R.-A., 2015. Cerebro-cerebellar resting-state functional connectivity in children and adolescents with autism spectrum disorder. Biol. Psychiatry 78 (9), 625–634. https://doi.org/10.1016/j.biopsych.2015.03.024.

Kim, H.-J., Cho, M.-H., Shim, W.H., Kim, J.K., Jeon, E.-Y., Kim, D.-H., Yoon, S.-Y., 2017. Deficient autophagy in microglia impairs synaptic pruning and causes social behavioral defects. Mol. Psychiatry 22 (11), 1576–1584. https://doi.org/10.1038/mp.2016.103.

Kong, X.-Z., Postema, M.C., Guadalupe, T., de Kovel, C., Boedhoe, P.S.W., Hoogman, M., Mathias, S.R., van Rooij, D., Schijven, D., Glahn, D.C., Medland, S.E., Jahanshad, N., Thomopoulos, S.I., Turner, J.A., Buitelaar, J., van Erp, T.G.M., Franke, B., Fisher, S.E., van den Heuvel, O.A., Schmaal, L., Thompson, P.M., Francks, C., 2020. Mapping brain asymmetry in health and disease through the ENIGMA consortium. Hum. Brain Mapp. https://doi.org/10.1002/hbm.25033.

Korgaonkar, M.S., Fornito, A., Williams, L.M., Grieve, S.M., 2014. Abnormal structural networks characterize major depressive disorder: a connectome analysis. Biol. Psychiatry 76 (7), 567–574. https://doi.org/10.1016/j.biopsych.2014.02.018.

Kravitz, D.J., Saleem, K.S., Baker, C.I., Mishkin, M., 2011. A new neural framework for visuospatial processing. Nat. Rev. Neurosci. 12 (4), 217–230. https://doi.org/10.1038/nrn3008.

Lahav, N., Ksherim, B., Ben-Simon, E., Maron-Katz, A., Cohen, R., Havlin, S., 2016. K-shell decomposition reveals hierarchical cortical organization of the human brain. New J. Phys. 18 (8), 083013. https://doi.org/10.1088/1367-2630/18/8/083013.

Laird, A.R., Fox, P.M., Price, C.J., Glahn, D.C., Uecker, A.M., Lancaster, J.L., Turkeltaub, P.E., Kochunov, P., Fox, P.T., 2005a. ALE meta-analysis: controlling the false discovery rate and performing statistical contrasts. Hum. Brain Mapp. 25 (1), 155–164. https://doi.org/10.1002/(ISSN)1097-019310.1002/hbm.v25:110.1002/hbm.20136.

Laird, A.R., Lancaster, J.L., Fox, P.T., 2005b. BrainMap: the social evolution of a human brain mapping database. Neuroinformatics 3 (1), 065–078. https://doi.org/10.1385/NI:3:110.1385/NI:3:1:065.

Laird, A.R., Robinson, J.L., McMillan, K.M., Tordesillas-Gutiérrez, D., Moran, S.T., Gonzales, S.M., Ray, K.L., Franklin, C., Glahn, D.C., Fox, P.T., Lancaster, J.L., 2010. Comparison of the disparity between Talairach and MNI coordinates in functional neuroimaging data: validation of the Lancaster transform. Neuroimage 51 (2), 677–683. https://doi.org/10.1016/j.neuroimage.2010.02.048.

Lancaster, J.L., Tordesillas-Gutiérrez, D., Martinez, M., Salinas, F., Evans, A., Zilles, K., Mazziotta, J.C., Fox, P.T., 2007. Bias between MNI and Talairach coordinates analyzed using the ICBM-152 brain template. Hum. Brain Mapp. 28 (11), 1194–1205. https://doi.org/10.1002/(ISSN)1097-019310.1002/hbm.v28:1110.1002/hbm.20345.

Lancaster, J.L., Woldorff, M.G., Parsons, L.M., Liotti, M., Freitas, C.S., Rainey, L., Kochunov, P.V., Nickerson, D., Mikiten, S.A., Fox, P.T., 2000. Automated Talairach atlas labels for functional brain mapping. Hum. Brain Mapp. 10, 120–131. https://doi.org/10.1002/1097-0193(200007)10:3<120::aid-hbm30>3.0.co;2-8.

Liang, X., Zou, Q., He, Y., Yang, Y., 2013. Coupling of functional connectivity and regional cerebral blood flow reveals a physiological basis for network hubs of the human brain. Proc. Natl. Acad. Sci. U.S.A. 110 (5), 1929–1934. https://doi.org/10.1073/pnas.1214900110.

Liberati, A., Altman, D.G., Tetzlaff, J., Mulrow, C., Gøtzsche, P.C., Ioannidis, J.P.A., Clarke, M., Devereaux, P.J., Kleijnen, J., Moher, D., 2009. The PRISMA statement for reporting systematic reviews and meta-analyses of studies that evaluate health care interventions: explanation and elaboration. J. Clin. Epidemiol. 62 (10), e1–e34. https://doi.org/10.1016/j.jclinepi.2009.06.006.

Liloia, D., Cauda, F., Nani, A., Manuello, J., Duca, S., Fox, P.T., Costa, T., 2018. Low entropy maps as patterns of the pathological alteration specificity of brain regions: a meta-analysis dataset. Data Brief 21, 1483–1495. https://doi.org/10.1016/j.dib.2018.10.142.

Liu, J., Yao, L., Zhang, W., Xiao, Y., Liu, L., Gao, X., Shah, C., Li, S., Tao, B., Gong, Q., Lui, S., 2017. Gray matter abnormalities in pediatric autism spectrum disorder: a meta-analysis with signed differential mapping. 26, 933-945. doi:10.1007/s00787-017-0964-4.

Lombardo, M.V., Eyler, L., Moore, A., Datko, M., Carter Barnes, C., Cha, D., Courchesne, E., Pierce, K., 2019. Default mode-visual network hypoconnectivity in an autism subtype with pronounced social visual engagement difficulties. Elife 8. https://doi.org/10.7554/eLife.47427.

Lord, C., Elsabbagh, M., Baird, G., Veenstra-Vanderweele, J., 2018. Autism spectrum disorder. Lancet 392 (10146), 508–520. https://doi.org/10.1016/S0140-6736(18)31129-2.

Lukito, S., Norman, L., Carlisi, C., Radua, J., Hart, H., Simonoff, E., Rubia, K., 2020. Comparative meta-analyses of brain structural and functional abnormalities during cognitive control in attention-deficit/hyperactivity disorder and autism spectrum disorder. Psychol. Med. 50 (6), 894–919. https://doi.org/10.1017/S0033291720000574.

Lynch, C.J., Uddin, L.Q., Supekar, K., Khouzam, A., Phillips, J., Menon, V., 2013. Default mode network in childhood autism: posteromedial cortex heterogeneity and relationship with social deficits. Biol. Psychiatry 74 (3), 212–219. https://doi.org/10.1016/j.biopsych.2012.12.013.

Mancuso, L., Costa, T., Nani, A., Manuello, J., Liloia, D., Gelmini, G., Panero, M., Duca, S., Cauda, F., 2019. The homotopic connectivity of the functional brain: a meta-analytic approach. Sci. Rep. 9, 3346. https://doi.org/10.1038/s41598-019-40188-3.

Mancuso, L., Fornito, A., Costa, T., Ficco, L., Liloia, D., Manuello, J., Duca, S., Cauda, F., 2020. A meta-analytic approach to mapping co-occurrent grey matter volume increases and decreases in psychiatric disorders. Neuroimage 222, 117220. https://doi.org/10.1016/j.neuroimage.2020.117220.

Mantel, N., 1967. The detection of disease clustering and a generalized regression approach. Cancer Res. 27, 209–220.

Manuello, J., Nani, A., Premi, E., Borroni, B., Costa, T., Tatu, K., Liloia, D., Duca, S., Cauda, F., 2018. The pathoconnectivity profile of Alzheimer's disease: a morphometric coalteration network analysis. Front. Neurol. 8 https://doi.org/10.3389/fneur.2017.00739.

Marco, E.J., Hinkley, L.B., Hill, S.S., Nagarajan, S.S., 2011. Sensory processing in autism: a review of neurophysiologic findings. Pediatr Res 69, 48r-54r. doi:10.1203/PDR.0b013e3182130c54.

Maslov, S., Sneppen, K., 2002. Specificity and Stability in Topology of Protein Networks. Science 296, 910–913. https://doi.org/10.1126/science.1065103.

Matsuoka, K., Makinodan, M., Kitamura, S., Takahashi, M., Yoshikawa, H., Yasuno, F., Ishida, R., Kishimoto, N., Yasuda, Y., Hashimoto, R., Taoka, T., Miyasaka, T., Kichikawa, K., Kishimoto, T., 2020. Increased Dendritic Orientation Dispersion in the Left Occipital Gyrus is Associated with Atypical Visual Processing in Adults with Autism Spectrum Disorder. Cereb Cortex. doi:10.1093/cercor/bhaa121.

Mellet, E., Zago, L., Jobard, G., Crivello, F., Petit, L., Joliot, M., Mazoyer, B., Tzourio-Mazoyer, N., 2014. Weak language lateralization affects both verbal and spatial skills: An fMRI study in 297 subjects. Neuropsychologia 65, 56–62. https://doi.org/10.1016/j.neuropsychologia.2014.10.010.

Minshew, N.J., Williams, D.L., 2007. The new neurobiology of autism: cortex, connectivity, and neuronal organization. Arch. Neurol. 64, 945–950. https://doi.org/10.1001/archneur.64.7.945.

Moher, D., Liberati, A., Tetzlaff, J., Altman, D.G., 2009. Preferred reporting items for systematic reviews and meta-analyses: the PRISMA statement. J. Clin. Epidemiol. 62 (10), 1006–1012. https://doi.org/10.1016/j.jclinepi.2009.06.005.

Morgan, J.T., Chana, G., Abramson, I., Semendeferi, K., Courchesne, E., Everall, I.P., 2012. Abnormal microglial-neuronal spatial organization in the dorsolateral prefrontal cortex in autism. Brain Res. 1456, 72–81. https://doi.org/10.1016/j.brainres.2012.03.036.

Muller, V.I., Cieslik, E.C., Laird, A.R., Fox, P.T., Radua, J., Mataix-Cols, D., Tench, C.R., Yarkoni, T., Nichols, T.E., Turkeltaub, P.E., Wager, T.D., Eickhoff, S.B., 2018. Ten simple rules for neuroimaging meta-analysis. Neurosci. Biobehav. Rev. 84, 151–161. https://doi.org/10.1016/j.neubiorev.2017.11.012.

Mundy, P., 2018. A review of joint attention and social-cognitive brain systems in typical development and autism spectrum disorder. Eur. J. Neurosci. 47 (6), 497–514. https://doi.org/10.1111/ejn.13720.

Nani, A., Manuello, J., Mancuso, L., Liloia, D., Costa, T., Vercelli, A., Duca, S., Cauda, F., 2021. The pathoconnectivity network analysis of the insular cortex: a morphometric fingerprinting. NeuroImage 225, 117481. https://doi.org/10.1016/j.neuroimage.2020.117481.

Nave, K.-A., 2010. Myelination and the trophic support of long axons. Nat. Rev. Neurosci. 11 (4), 275–283. https://doi.org/10.1038/nrn2797.

Neniskyte, U., Gross, C.T., 2017. Errant gardeners: glial-cell-dependent synaptic pruning and neurodevelopmental disorders. Nat. Rev. Neurosci. 18 (11), 658–670. https://doi.org/10.1038/nrn.2017.110.

Nickl-Jockschat, T., Habel, U., Maria Michel, T., Manning, J., Laird, A.R., Fox, P.T., Schneider, F., Eickhoff, S.B., 2012. Brain structure anomalies in autism spectrum disorder–a meta-analysis of VBM studies using anatomic likelihood estimation. Hum. Brain Mapp. 33 (6), 1470–1489. https://doi.org/10.1002/hbm.v33.610.1002/hbm.21299.

Nickl-Jockschat, T., Michel, T.M., 2011. The role of neurotrophic factors in autism. Mol. Psychiatry 16 (5), 478–490. https://doi.org/10.1038/mp.2010.103.

Nieto Del Rincón, P.L., 2008. Autism: alterations in auditory perception. Rev. Neurosci. 19, 61–78. https://doi.org/10.1515/revneuro.2008.19.1.61.

Nomi, J.S., Uddin, L.Q., 2015. Developmental changes in large-scale network connectivity in autism. Neuroimage Clin 7, 732–741. https://doi.org/10.1016/j.nicl.2015.02.024.

Noonan, S.K., Haist, F., Muller, R.A., 2009. Aberrant functional connectivity in autism: evidence from low-frequency BOLD signal fluctuations. Brain Res. 1262, 48–63. https://doi.org/10.1016/j.brainres.2008.12.076.

Norman, L.J., Carlisi, C., Lukito, S., Hart, H., Mataix-Cols, D., Radua, J., Rubia, K., 2016. Structural and Functional Brain Abnormalities in Attention-Deficit/Hyperactivity Disorder and Obsessive-Compulsive Disorder: A Comparative Meta-analysis. JAMA Psychiatry 73, 815–825. https://doi.org/10.1001/jamapsychiatry.2016.0700.

Padmanabhan, A., Lynch, C.J., Schaer, M., Menon, V., 2017. The Default Mode Network in Autism. Biological Psychiatry: Cognitive Neuroscience and Neuroimaging 2 (6), 476–486. https://doi.org/10.1016/j.bpsc.2017.04.004.

Palande, S., Jose, V., Zielinski, B., Anderson, J., Fletcher, P.T., Wang, B., 2017. Revisiting Abnormalities in Brain Network Architecture Underlying Autism Using Topology-Inspired Statistical Inference. Connectomics Neuroimaging 2017 (10511), 98–107. https://doi.org/10.1007/978-3-319-67159-8_12.

Palmen, S.J., van Engeland, H., Hof, P.R., Schmitz, C., 2004. Neuropathological findings in autism. Brain 127, 2572–2583. https://doi.org/10.1093/brain/awh287.

Pappaianni, E., Siugzdaite, R., Vettori, S., Venuti, P., Job, R., Grecucci, A., 2018. Three shades of grey: detecting brain abnormalities in children with autism using source-, voxel- and surface-based morphometry. Eur. J. Neurosci. 47 (6), 690–700. https://doi.org/10.1111/ejn.13704.

Patel, R.S., Bowman, F.D., Rilling, J.K., 2006. A Bayesian approach to determining connectivity of the human brain. Hum. Brain Mapp. 27 (3), 267–276. https://doi.org/10.1002/(ISSN)1097-019310.1002/hbm.v27:310.1002/hbm.20182.

Patriquin, M.A., DeRamus, T., Libero, L.E., Laird, A., Kana, R.K., 2016. Neuroanatomical and neurofunctional markers of social cognition in autism spectrum disorder. Hum. Brain Mapp. 37 (11), 3957–3978. https://doi.org/10.1002/hbm.v37.1110.1002/hbm.23288.

Perlson, E., Maday, S., Fu, M.-M., Moughamian, A.J., Holzbaur, E.L.F., 2010. Retrograde axonal transport: pathways to cell death? Trends Neurosci. 33 (7), 335–344. https://doi.org/10.1016/j.tins.2010.03.006.

Picci, G., Gotts, S.J., Scherf, K.S., 2016. A theoretical rut: revisiting and critically evaluating the generalized under/over-connectivity hypothesis of autism. Dev Sci 19 (4), 524–549. https://doi.org/10.1111/desc.2016.19.issue-410.1111/desc.12467.

Postema, M.C., van Rooij, D., Anagnostou, E., Arango, C., Auzias, G., Behrmann, M., Filho, G.B., Calderoni, S., Calvo, R., Daly, E., Deruelle, C., Di Martino, A., Dinstein, I., Duran, F.L.S., Durston, S., Ecker, C., Ehrlich, S., Fair, D., Fedor, J., Feng, X., Fitzgerald, J., Floris, D.L., Freitag, C.M., Gallagher, L., Glahn, D.C., Gori, I., Haar, S., Hoekstra, L., Jahanshad, N., Jalbrzikowski, M., Janssen, J., King, J.A., Kong, X.Z., Lazaro, L., Lerch, J.P., Luna, B., Martinho, M.M., McGrath, J., Medland, S.E., Muratori, F., Murphy, C.M., Murphy, D.G.M., O'Hearn, K., Oranje, B., Parellada, M., Puig, O., Retico, A., Rosa, P., Rubia, K., Shook, D., Taylor, M.J., Tosetti, M., Wallace, G.L., Zhou, F., Thompson, P.M., Fisher, S.E., Buitelaar, J.K., Francks, C., 2019. Altered structural brain asymmetry in autism spectrum disorder in a study of 54 datasets. Nat. Commun. 10 (1) https://doi.org/10.1038/s41467-019-13005-8.

Prior, M.R., Bradshaw, J.L., 1979. Hemisphere functioning in autistic children. Cortex 15 (1), 73–81. https://doi.org/10.1016/S0010-9452(79)80008-8.

Qin, X.Y., Feng, J.C., Cao, C., Wu, H.T., Loh, Y.P., Cheng, Y., 2016. Association of Peripheral Blood Levels of Brain-Derived Neurotrophic Factor With Autism Spectrum Disorder in Children: A Systematic Review and Meta-analysis. JAMA Pediatr 170, 1079–1086. https://doi.org/10.1001/jamapediatrics.2016.1626.

Qiu, A., Adler, M., Crocetti, D., Miller, M.I., Mostofsky, S.H., 2010. Basal ganglia shapes predict social, communication, and motor dysfunctions in boys with autism spectrum disorder. J Am Acad Child Adolesc Psychiatry 49, 539-551, 551.e531-534. doi:10.1016/j.jaac.2010.02.012.

Raj, A., Kuceyeski, A., Weiner, M., 2012. A network diffusion model of disease progression in dementia. Neuron 73 (6), 1204–1215. https://doi.org/10.1016/j.neuron.2011.12.040.

Raj, A., Powell, F., 2018. Models of Network Spread and Network Degeneration in Brain Disorders. Biol Psychiatry Cogn Neurosci Neuroimaging 3 (9), 788–797. https://doi.org/10.1016/j.bpsc.2018.07.012.

Reess, T.J., Rus, O.G., Schmidt, R., de Reus, M.A., Zaudig, M., Wagner, G., Zimmer, C., van den Heuvel, M.P., Koch, K., 2016. Connectomics-based structural network alterations in obsessive-compulsive disorder. e882 Transl. Psychiatry 6 (9), e882. https://doi.org/10.1038/tp.2016.163.

Robertson, C.E., Baron-Cohen, S., 2017. Sensory perception in autism. Nat. Rev. Neurosci. 18 (11), 671–684. https://doi.org/10.1038/nrn.2017.112.

Rolls, E.T., 2019. The cingulate cortex and limbic systems for emotion, action, and memory. Brain Struct. Funct. 224 (9), 3001–3018. https://doi.org/10.1007/s00429-019-01945-2.

Rubinov, M., Bullmore, E.d., 2013. Fledgling pathoconnectomics of psychiatric disorders. Trends Cogn Sci 17 (12), 641–647. https://doi.org/10.1016/j.tics.2013.10.007.
Rubinov, M., Sporns, O., 2010. Complex network measures of brain connectivity: uses and interpretations. Neuroimage 52 (3), 1059–1069. https://doi.org/10.1016/j.neuroimage.2009.10.003.
Salehi, A., Delcroix, J.-D., Mobley, W.C., 2003. Traffic at the intersection of neurotrophic factor signaling and neurodegeneration. Trends Neurosci. 26 (2), 73–80. https://doi.org/10.1016/S0166-2236(02)00038-3.
Scardoni, G., Tosadori, G., Faizan, M., Spoto, F., Fabbri, F., Laudanna, C., 2014. Biological network analysis with CentiScaPe: centralities and experimental dataset integration. F1000Res 3, 139. doi:10.12688/f1000research.4477.2.
Schaefer, A., Kong, R., Gordon, E.M., Laumann, T.O., Zuo, X.N., Holmes, A.J., Eickhoff, S. B., Yeo, B.T.T., 2018. Local-Global Parcellation of the Human Cerebral Cortex from Intrinsic Functional Connectivity MRI. Cereb. Cortex 28, 3095–3114. https://doi.org/10.1093/cercor/bhx179.
Schaer, M., Ottet, M.-C., Scariati, E., Dukes, D., Franchini, M., Eliez, S., Glaser, B., 2013. Decreased frontal gyrification correlates with altered connectivity in children with autism. Front. Hum. Neurosci. 7 https://doi.org/10.3389/fnhum.2013.00750.
Schulte-Rüther, M., Greimel, E., Markowitsch, H.J., Kamp-Becker, I., Remschmidt, H., Fink, G.R., Piefke, M., 2011. Dysfunctions in brain networks supporting empathy: an fMRI study in adults with autism spectrum disorders. Soc. Neurosci. 6 (1), 1–21. https://doi.org/10.1080/17470911003708032.
Shafiei, G., Markello, R.D., Makowski, C., Talpalaru, A., Kirschner, M., Devenyi, G.A., Guma, E., Hagmann, P., Cashman, N.R., Lepage, M., Chakravarty, M.M., Dagher, A., Mišić, B., 2020. Spatial Patterning of Tissue Volume Loss in Schizophrenia Reflects Brain Network Architecture. Biol. Psychiatry 87 (8), 727–735. https://doi.org/10.1016/j.biopsych.2019.09.031.
Sharda, M., Foster, N.E.V., Tryfon, A., Doyle-Thomas, K.A.R., Ouimet, T., Anagnostou, E., Evans, A.C., Zwaigenbaum, L., Lerch, J.P., Lewis, J.D., Hyde, K.L., 2017. Language Ability Predicts Cortical Structure and Covariance in Boys with Autism Spectrum Disorder. Cereb. Cortex 27, 1849–1862. https://doi.org/10.1093/cercor/bhw024.
Smith, S.M., Miller, K.L., Salimi-Khorshidi, G., Webster, M., Beckmann, C.F., Nichols, T. E., Ramsey, J.D., Woolrich, M.W., 2011. Network modelling methods for FMRI. Neuroimage 54 (2), 875–891. https://doi.org/10.1016/j.neuroimage.2010.08.063.
Sporns, O., 2013. The human connectome: origins and challenges. Neuroimage 80, 53–61. https://doi.org/10.1016/j.neuroimage.2013.03.023.
Stam, C.J., 2014. Modern network science of neurological disorders. Nat. Rev. Neurosci. 15 (10), 683–695. https://doi.org/10.1038/nrn3801.
Stevens, F.L., Hurley, R.A., Taber, K.H., Hurley, R.A., Hayman, L.A., Taber, K.H., 2011. Anterior cingulate cortex: unique role in cognition and emotion. J. Neuropsychiatry Clin. Neurosci. 23 (2), 121–125. https://doi.org/10.1176/jnp.23.2.jnp121.
Su, G., Morris, J.H., Demchak, B., Bader, G.D., 2014. Biological network exploration with Cytoscape 3. Curr Protoc Bioinformatics 47, 8.13.11-24. https://doi.org/10.1002/0471250953.bi0813s47.
Tahmasian, M., Sepehry, A.A., Samea, F., Khodadadifar, T., Soltaninejad, Z., Javaheripour, N., Khazaie, H., Zarei, M., Eickhoff, S.B., Eickhoff, C.R., 2019. Practical recommendations to conduct a neuroimaging meta-analysis for neuropsychiatric disorders. Hum. Brain Mapp. 40 (17), 5142–5154. https://doi.org/10.1002/hbm.v40.1710.1002/hbm.24746.
Tatu, K., Costa, T., Nani, A., Diano, M., Quarta, D.G., Duca, S., Apkarian, A.V., Fox, P.T., Cauda, F., 2018. How do morphological alterations caused by chronic pain distribute across the brain? A meta-analytic co-alteration study. NeuroImage: Clinical 18, 15–30. https://doi.org/10.1016/j.nicl.2017.12.029.
Thomas, M.S.C., Davis, R., Karmiloff-Smith, A., Knowland, V.C.P., Charman, T., 2016. The over-pruning hypothesis of autism. Dev Sci 19 (2), 284–305. https://doi.org/10.1111/desc.2016.19.issue-210.1111/desc.12303.
Turner, K.C., Frost, L., Linsenbardt, D., McIlroy, J.R., Müller, R.-A., 2006. Atypically diffuse functional connectivity between caudate nuclei and cerebral cortex in autism. Behavioral and Brain Functions 2, 34. https://doi.org/10.1186/1744-9081-2-34.
Uddin, L.Q., 2015. Salience processing and insular cortical function and dysfunction. Nat. Rev. Neurosci. 16 (1), 55–61. https://doi.org/10.1038/nrn3857.
Uddin, L.Q., Supekar, K., Menon, V., 2013. Reconceptualizing functional brain connectivity in autism from a developmental perspective. Front. Hum. Neurosci. 7 https://doi.org/10.3389/fnhum.2013.00458.
Valente, T.W., Coronges, K., Lakon, C., Costenbader, E., 2008. How correlated are network centrality measures? Connections (Toronto, Ont.) 28, 16.
Valk, S.L., Di Martino, A., Milham, M.P., Bernhardt, B.C., 2015. Multicenter mapping of structural network alterations in autism. Hum. Brain Mapp. 36 (6), 2364–2373. https://doi.org/10.1002/hbm.22776.
van den Heuvel, M.P., Mandl, R.C.W., Stam, C.J., Kahn, R.S., Hulshoff Pol, H.E., 2010. Aberrant frontal and temporal complex network structure in schizophrenia: a graph theoretical analysis. J. Neurosci. 30 (47), 15915–15926. https://doi.org/10.1523/JNEUROSCI.2874-10.2010.
van den Heuvel, M.P., Sporns, O., 2013. Network hubs in the human brain. Trends Cogn Sci 17 (12), 683–696. https://doi.org/10.1016/j.tics.2013.09.012.
van den Heuvel, M.P., Sporns, O., 2019. A cross-disorder connectome landscape of brain dysconnectivity. Nat. Rev. Neurosci. 20 (7), 435–446. https://doi.org/10.1038/s41583-019-0177-6.
Van Essen, D.C., Smith, S.M., Barch, D.M., Behrens, T.E., Yacoub, E., Ugurbil, K., 2013. The WU-Minn Human Connectome Project: an overview. Neuroimage 80, 62–79. https://doi.org/10.1016/j.neuroimage.2013.05.041.
Vanasse, T.J., Fox, P.M., Barron, D.S., Robertson, M., Eickhoff, S.B., Lancaster, J.L., Fox, P.T., 2018. BrainMap VBM: An environment for structural meta-analysis. Hum. Brain Mapp. 39 (8), 3308–3325. https://doi.org/10.1002/hbm.v39.810.1002/hbm.24078.
Verly, M., Verhoeven, J., Zink, I., Mantini, D., Peeters, R., Deprez, S., Emsell, L., Boets, B., Noens, I., Steyaert, J., Lagae, L., De Cock, P., Rommel, N., Sunaert, S., 2014. Altered functional connectivity of the language network in ASD: role of classical language areas and cerebellum. Neuroimage Clin 4, 374–382. https://doi.org/10.1016/j.nicl.2014.01.008.
Via, E., Radua, J., Cardoner, N., Happe, F., Mataix-Cols, D., 2011. Meta-analysis of gray matter abnormalities in autism spectrum disorder: should Asperger disorder be subsumed under a broader umbrella of autistic spectrum disorder? Arch. Gen. Psychiatry 68, 409–418. https://doi.org/10.1001/archgenpsychiatry.2011.27.
von dem Hagen, E.A., Stoyanova, R.S., Baron-Cohen, S., Calder, A.J., 2013. Reduced functional connectivity within and between 'social' resting state networks in autism spectrum conditions. Soc Cogn Affect Neurosci 8, 694–701. https://doi.org/10.1093/scan/nss053.
Wang, A.T., Lee, S.S., Sigman, M., Dapretto, M., 2007. Reading affect in the face and voice: neural correlates of interpreting communicative intent in children and adolescents with autism spectrum disorders. Arch. Gen. Psychiatry 64, 698–708. https://doi.org/10.1001/archpsyc.64.6.698.
Ward, A.M., Schultz, A.P., Huijbers, W., Van Dijk, K.R.A., Hedden, T., Sperling, R.A., 2014. The parahippocampal gyrus links the default-mode cortical network with the medial temporal lobe memory system. Hum. Brain Mapp. 35 (3), 1061–1073. https://doi.org/10.1002/hbm.22234.
Wegiel, J., Flory, M., Kuchna, I., Nowicki, K., Ma, S.Y., Imaki, H., Wegiel, J., Cohen, I.L., London, E., Brown, W.T., Wisniewski, T., 2014. Brain-region-specific alterations of the trajectories of neuronal volume growth throughout the lifespan in autism. Acta Neuropathol Commun 2, 28. https://doi.org/10.1186/2051-5960-2-28.
Williams, Z.J., He, J.L., Cascio, C.J., Woynaroski, T.G., 2021. A Review of Decreased Sound Tolerance in Autism: Definitions, Phenomenology, and Potential Mechanisms. Neurosci. Biobehav. Rev. 121, 1–17. https://doi.org/10.1016/j.neubiorev.2020.11.030.
Worbe, Y., 2015. Neuroimaging signature of neuropsychiatric disorders. Curr. Opin. Neurol. 28 (4), 358–364. https://doi.org/10.1097/WCO.0000000000000220.
Wylie, K.P., Tregellas, J.R., Bear, J.J., Legget, K.T., 2020. Autism Spectrum Disorder Symptoms are Associated with Connectivity Between Large-Scale Neural Networks and Brain Regions Involved in Social Processing. J. Autism Dev. Disord. 50 (8), 2765–2778. https://doi.org/10.1007/s10803-020-04383-w.
Xia, M., Wang, J., He, Y., Csermely, P., 2013. BrainNet Viewer: a network visualization tool for human brain connectomics. PLoS ONE 8 (7), e68910. https://doi.org/10.1371/journal.pone.0068910.
Yahata, N., Kasai, K., Kawato, M., 2017. Computational neuroscience approach to biomarkers and treatments for mental disorders. Psychiatry Clin. Neurosci. 71 (4), 215–237. https://doi.org/10.1111/pcn.2017.71.issue-410.1111/pcn.12502.
Yeh, F.-C., Tseng, W.-Y., 2011. NTU-90: a high angular resolution brain atlas constructed by q-space diffeomorphic reconstruction. Neuroimage 58 (1), 91–99. https://doi.org/10.1016/j.neuroimage.2011.06.021.
Yeh, F.C., Wedeen, V.J., Tseng, W.Y., 2010. Generalized q-sampling imaging. IEEE Trans. Med. Imaging 29, 1626–1635. https://doi.org/10.1109/tmi.2010.2045126.
Thomas Yeo, B.T., Krienen, F.M., Sepulcre, J., Sabuncu, M.R., Lashkari, D., Hollinshead, M., Roffman, J.L., Smoller, J.W., Zöllei, L., Polimeni, J.R., Fischl, B., Liu, H., Buckner, R.L., 2011. The organization of the human cerebral cortex estimated by intrinsic functional connectivity. J. Neurophysiol. 106 (3), 1125–1165. https://doi.org/10.1152/jn.00338.2011.
Zhang, S., Li, C.-S., 2012. Functional connectivity mapping of the human precuneus by resting state fMRI. Neuroimage 59 (4), 3548–3562. https://doi.org/10.1016/j.neuroimage.2011.11.023.
Zheng, K., Wang, H., Li, J., Yan, B., Liu, J., Xi, Y., Zhang, X., Yin, H., Tan, Q., Lu, H., Li, B., 2019. Structural networks analysis for depression combined with graph theory and the properties of fiber tracts via diffusion tensor imaging. Neurosci. Lett. 694, 34–40. https://doi.org/10.1016/j.neulet.2018.11.025.
Zheng, W., Zhao, Z., Zhang, Z., Liu, T., Zhang, Y., Fan, J., Wu, D., 2020. Developmental pattern of the cortical topology in high-functioning individuals with autism spectrum disorder. Hum Brain Mapp n/a. https://doi.org/10.1002/hbm.25251.
Zheng, Z., Zhang, L., Zhu, T., Huang, J., Qu, Y., Mu, D., 2016. Peripheral brain-derived neurotrophic factor in autism spectrum disorder: a systematic review and meta-analysis. Sci. Rep. 6, 31241. https://doi.org/10.1038/srep31241.
Zhou, J., Gennatas, E., Kramer, J., Miller, B., Seeley, W., 2012. Predicting regional neurodegeneration from the healthy brain functional connectome. Neuron 73 (6), 1216–1227. https://doi.org/10.1016/j.neuron.2012.03.004.
Zhou, Y., Shi, L., Cui, X., Wang, S., Luo, X., Stamatakis, E.A., 2016. Functional Connectivity of the Caudal Anterior Cingulate Cortex Is Decreased in Autism. PLoS ONE 11 (3), e0151879. https://doi.org/10.1371/journal.pone.0151879.
Zielinski, B.A., Anderson, J.S., Froehlich, A.L., Prigge, M.B.D., Nielsen, J.A., Cooperrider, J.R., Cariello, A.N., Fletcher, P.T., Alexander, A.L., Lange, N., Bigler, E. D., Lainhart, J.E., Soriano-Mas, C., 2012. scMRI reveals large-scale brain network abnormalities in autism. PLoS ONE 7 (11), e49172. https://doi.org/10.1371/journal.pone.0049172.